

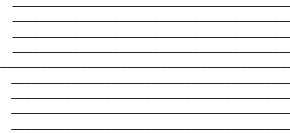
The Impact of Freshwater Forcing on a University of Toronto Model for Dansgaard-Oeschger Oscillations

by

George Lu

Supervisor: Prof. W.R. Peltier
April 2021

B.A.Sc. Thesis



Division of Engineering Science
UNIVERSITY OF TORONTO

The Impact of Freshwater Forcing on a University of
Toronto Model for Dansgaard-Oeschger Oscillations
A B.A.Sc Thesis Project

By: George Lu (1003063490)
Supervisor: Prof. W.R. Peltier
ESC 499
April 2021

Abstract

Dansgaard-Oeschger oscillations (D-O oscillations) are millennial scale oscillations in temperature identified in various paleoclimate proxies surrounding the North Atlantic. These oscillations are tied to variations in the Atlantic Meridional Overturning Circulation (AMOC), a circulation pattern that still impacts the climate today. Various climate models have been used to get a better understanding of the underlying mechanisms behind D-O oscillations. One significant model is the UofT-CCSM4 model, which is the first fully coupled, high resolution global climate model to create D-O-like oscillations. Furthermore, it did not require any freshwater forcing to do so, a process which was thought to be indispensable in previous models. However, these oscillations in the UofT-CCSM4 model differ from D-O oscillations in that they have an "infinite-Q" – the periods and amplitudes of each pulse remain the same, whereas the oscillations in ice core records decrease in period and amplitude with each subsequent pulse, thus having a "finite-Q". The goal of this project was to see if additional freshwater forcing in the UofT-CCSM4 model could shape these pulses to have the reduced amplitudes and periods that result in a "finite-Q". By applying varying amounts of freshwater forcing at different times directly to the North Atlantic, this project was able to identify a range of forcing levels that can shape the D-O pulses. However, it cannot concretely conclude that this forcing is the mechanism behind the "finite-Q", so it offers a starting block for additional investigations.

Acknowledgements

First and foremost, I'd like to thank Prof. W.R. Peltier for giving me the opportunity to conduct work with him, for his patience and time, and for his indispensable knowledge on the subject. He granted me access to SciNet, which was instrumental for the running of my simulations. His climate dynamics course also furthered my interests in climate physics and paleoclimate. Next, a thank you is in order for Dr. Deepak Chandan and Jesse Velay-Vitow for their insights and aid throughout the project. Dr. Chandan taught me how to run simulations and provided the necessary scripts and tips.

This project was conducted during a unique time, and the COVID-19 pandemic certainly made research, school, and life in general quite tricky at times. Consequently, I must acknowledge those who have helped me stay optimistic throughout my undergraduate career, especially during this final stretch. This includes my friends, my classmates, and my family. Dr. Chandan deserves another acknowledgement in this aspect for his reassurance and his guidance throughout the project.

Finally, I'd like to thank the University of Toronto, its facilities, and its faculty for fostering the learning experiences I've had. In specific, the Department of Engineering Science has given me great opportunities and challenges that have strongly shaped my career. Above all, I'd like to thank my parents, Mr. Zhongxue Lu and Mrs. Yuhui Liu, for their unwavering support and faith in me.

Table of Contents

List of Figures	iv
List of Tables	v
1. Introduction	1
2. Background on D-O Oscillations	3
2.1 Understanding Paleoclimate Proxies	3
2.2 Identification of D-O Oscillations	4
2.3 The Atlantic Meridional Overturning Circulation	5
2.4 Description of Interstadials	9
2.5 Description of D-O Stadials	10
2.6 Description of Heinrich Events	11
2.7 Mechanisms	14
3. Background on Climate Modelling	17
3.1 A History of Climate Modelling	17
3.2 Modelling D-O Oscillations	20
3.3 The UofT-CCSM4 Model	21
3.4 Experiment opportunity	23
4. Methods	25
5. Results	27
5.1 Freshwater forcing of 0.2 Sv (v1)	27
5.2 Freshwater forcing of 0.1 Sv (v2)	29
5.3 Freshwater forcing of 0.01 Sv (v3)	34
6. Discussion	37
7. Conclusions	40
8. References	41
9. Appendices	48
A. Some technical information about SciNet	48
B. Workflow for running simulations (Detailed Method)	49
C. Code snippets for plotting	52

List of Figures

Figure 1: D-O oscillations from MIS 1-5	5
Figure 2: Sketch of global overturning circulation	6
Figure 3: Different AMOC modes	8
Figure 4: Comparison of WAIS ice core to NGRIP ice core	11
Figure 5: Map of Ruddiman belt	12
Figure 6: D-O oscillations over last glacial cycle with labelled Heinrich events	13
Figure 7: Differences between D-O stadials and Heinrich stadials	13
Figure 8: Proposed mechanisms for D-O oscillations	16
Figure 9: History of model complexity	18
Figure 10: History of model resolution	19
Figure 11: Simulated AMOC strength from Peltier et al. (2020)	23
Figure 12: All simulated AMOC strengths compared with Peltier et al. (2020)	25
Figure 13: Area of forcing for project	26
Figure 14: Simulated AMOC strength in v1	27
Figure 15: Simulated temperatures at NGRIP and EDML in v1	28
Figure 16: Simulated AMOC strength in v2	29
Figure 17: Simulated temperatures at NGRIP and EDML in v2	30
Figure 18: Temperature anomalies between noDD and v2 overshoots	31
Figure 19: Shifted v2 time series aligning the second pulse peak	32
Figure 20: Temperature anomalies between v2 stadials	33
Figure 21: Simulated AMOC strength in v3	34
Figure 22: Temperature anomalies between v3 and noDD stadials	36
Figure 23: Simulated temperatures at NGRIP and EDML in v3	36
Figure 24: Proposed time-varying forcing shape	39

List of Tables

Table 1: Components of CCSM4 utilized in UofT-CCSM4	22
Table 2: Summary of forcing and timing details for each simulation	22
Table B1: Specified build configuration parameters for project models	48

1. Introduction

Dansgaard-Oeschger oscillations (D-O oscillations) are frequently used as a paleoclimate example of rapid climate change. They consist of millennial scale oscillations between warm interstadial conditions and cold stadial conditions and were first identified in Greenland ice cores by Willi Dansgaard and colleagues, though their signatures can be seen throughout the North Atlantic (Dansgaard et al., 1969, Oeschger et al., 1984). The study of the mechanisms behind these events allows for many general insights into the mechanisms driving global climate as a whole. Furthermore, they offer a natural example to test the rigour of climate models, especially with regards to their ability to pre-emptively identify the potential for future sudden climate changes in response to sustained long-term anthropogenic warming. It is important to have a better understanding of these phenomena since understanding the climate of the past can help one understand the climate of today and even make predictions about future climatic changes. For example, we are currently undergoing rapid climate change due to anthropogenic forcing, and climate modelling has become the primary avenue for setting and evaluating climate goals. With these unprecedented shifts in climate, a good method of getting a better understanding of how the climate might behave would be to look at historical instances of rapid climate change, of which D-O oscillations are an example. In the fourth assessment report by the Intergovernmental Panel on Climate Change (IPCC), it was noted that although past climates may not be exact analogues of what is to come, they provide key insights on climate processes that will help better project climate change in the future (Le Treut et al., 2007). Consequently, IPCC's latest report (AR5) has an entire chapter dedicated to the significance of both data from paleoclimate archives and climate modelling (IPCC, 2013).

In the ongoing efforts to understand D-O oscillations with climate models, one model has stood out in its ability to reproduce salient features of D-O oscillations and provide insights into its mechanisms: the University of Toronto version of the National Center for Atmospheric Research CCSM4 global model (UofT-CCSM4; Peltier and Vettoretti, 2014). One significant aspect of this model's results was the demonstration that the simulated D-O oscillations involved a “kicked” salt oscillator, where a pseudo-Heinrich event (mimicking a real Heinrich event which involves large ice-raftering event in the North Atlantic) provides the “kick” to the Atlantic Meridional Overturning Circulation (AMOC) (Peltier and Vettoretti, 2014). The subsequent

oscillatory behaviour of the AMOC is then akin to D-O oscillations (Peltier and Vettoretti, 2014). A further significant feature of this model is that it does not utilize freshwater forcing, which was previously thought to be required for the simulation of D-O oscillations (Knutti et al., 2004).

Discussions further in this report will highlight that there still remain several unanswered questions about the results from this model. First, the UofT-CCSM4 model observes a perfectly in-phase relationship between peak warming periods in the Northern and Southern Hemispheres, which contrasts with existing studies that estimate a time lag (Peltier et al., 2020; WAIS, 2015). Furthermore, the periods and the amplitudes of the modelled D-O oscillations do not decrease with each oscillation, which is a feature that is observed within the ice cores (Peltier et al., 2020). A possible reason behind these discrepancies could be that the UofT-CCSM4 model does not incorporate any freshwater forcing, and therefore neglects potential freshwater exchange between continents and the oceans during the warm phases of the oscillations (Peltier et al., 2020).

These unanswered questions that arise from the UofT-CCSM4 model results could potentially be answered by investigating the interaction between additional freshwater forcing and the AMOC, a factor that is currently neglected. This opportunity for investigation forms the basis for this thesis project. Therefore, the main goal for this project is to add freshwater forcing to the existing D-O oscillation model, and to analyze the subsequent model results. This project is scoped to three simulations, each with different freshwater forcing amounts applied at different times to get a sense of the impact of freshwater forcing. The results from the three simulations present an understanding of how freshwater forcing can shape the pulses and offer a range of forcing values that can impart significant impact to the AMOC. However, as noted in the discussion, there is still many factors left to explore, including the size, shape, and area of the freshwater forcing. Overall, this project acts as a starting block for further investigations on freshwater forcing effects on D-O oscillation pulse shape by providing an initial understanding of how the pulse shapes can be altered.

2. Background on D-O Oscillations

2.1 Understanding paleoclimate proxies

The evidence for D-O oscillations is most prominent in ice cores taken from the Greenland ice sheet. In order to understand how these oscillations are observed in the ice cores, one first must understand paleoclimate proxies, notably the temperature proxy that is $\delta^{18}\text{O}$ through which these oscillations were first recorded. $\delta^{18}\text{O}$ is the ratio between two different oxygen isotopes that could form water molecules, the more commonly occurring O^{16} isotope and the less common O^{18} isotope. In 1954, Wili Dansgaard demonstrated how this ratio is directly correlated to precipitation temperature. This linear relationship is shown through a reduction in O^{18} as temperatures drop. This is due to the nature of these two isotopes: O^{18} is heavier than O^{16} , so it evaporates less readily than its lighter counterpart. These isotopes circulate by evaporating from the ocean into the atmosphere, moving towards higher latitudes, and as it moves and cools, begin precipitating out (Dansgaard, 1954). Since O^{18} is heavier, it precipitates out first. This movement can be observed through drops in the abundance of O^{18} in areas of increasing latitudes (Dansgaard, 1954). Therefore, it can be assumed that during ice ages, when colder temperatures extend to lower latitudes, even more O^{18} condenses out before reaching the poles, so there is even less O^{18} found in the ice. In his paper detailing the use of $\delta^{18}\text{O}$ as a temperature proxy, Dansgaard (1954) proposes using this technique in cores taken from the Greenland ice sheet as distinct yearly layers can be identified within those cores. This is due to higher dust content in summers which results in those layers scattering more light than the winter layers, which appear darker in images (Meese et al., 1997). With these layers, a long climate record can be determined; for example, the Greenland Ice Core Project (GRIP) produced a 250 kyr record from a 3000 m long core (Dansgaard et al., 1993). This logic also applies to trapped oxygen isotopes from marine sediment cores (which can get trapped by microorganisms like planktonic foraminifera) – a colder climate would imply an increase in O^{18} in marine sediment cores as less would evaporate out and get trapped in the ice sheets. An example of a marine core providing insights into past climates can be found by Hartmut Heinrich's analysis of deep-sea sediment cores (utilizing planktonic foraminifera in addition to ice-raftered debris) from the Northeast Atlantic Ocean which ultimately resulted in the identification of large ice rafting events that will later be dubbed as Heinrich events (Heinrich, 1988). There exist many other paleoclimatic proxies that can reveal insights on other factors of climate outside of temperature, but throughout

this project, the main comparisons are with the temperature profiles or $\delta^{18}\text{O}$ profiles pulled from polar ice cores.

2.2 Identification of D-O oscillations

Over the course of the last glacial-interglacial cycle, 25 D-O oscillations have been observed in the Greenland ice core record (North Greenland Ice Core Project members, 2004). A large number of those oscillations (15) are observed during Marine Isotope Stage 3 (MIS 3), which lasted from about 60,000 years BP to 24,000 years BP (Wolff et al., 2010). All D-O oscillations recorded in the North Greenland Ice core Project (NGRIP) core over the last glacial cycle are individually identified in Figure 1 (Wolff et al., 2010). Prior to the NGRIP core, other significant cores taken from Greenland were the GRIP core mentioned earlier, and the Camp Century core in which Dansgaard et al. (1969) first noted violent fluctuations in $\delta^{18}\text{O}$ that would later be dubbed D-O events. Another set of cores drilled in 1981 in Greenland allowed Dansgaard et al. (1982) to verify that these fluctuations in $\delta^{18}\text{O}$ were not just local but were representative of large shifts in climate throughout the Northern Hemisphere. This core profile was also compared to lake carbonate cores by Oeschger et al. (1984) to further realize the widespread nature of these oscillations. Throughout these cores, the D-O oscillations are seen as millennial scale oscillations between cold “stadials” and warm “interstadials”. Oeschger et al. also noted a concurrent fluctuation in carbon dioxide, which they attributed to changes in ocean circulation (Oeschger et al., 1984). Similar fluctuations in temperature were found in faunal and $\delta^{18}\text{O}$ records taken from the Norwegian sea, which suggested large sea surface temperature shifts of over 5°C in less than 40 years (Lehman and Keigwin, 1992). The nature of these oscillations and additional evidence will be examined further, but first it must be noted that a linkage can already be seen between D-O oscillations and ocean circulation. Thus, the following section will examine this linkage between large climate fluctuations and changes in ocean circulation.

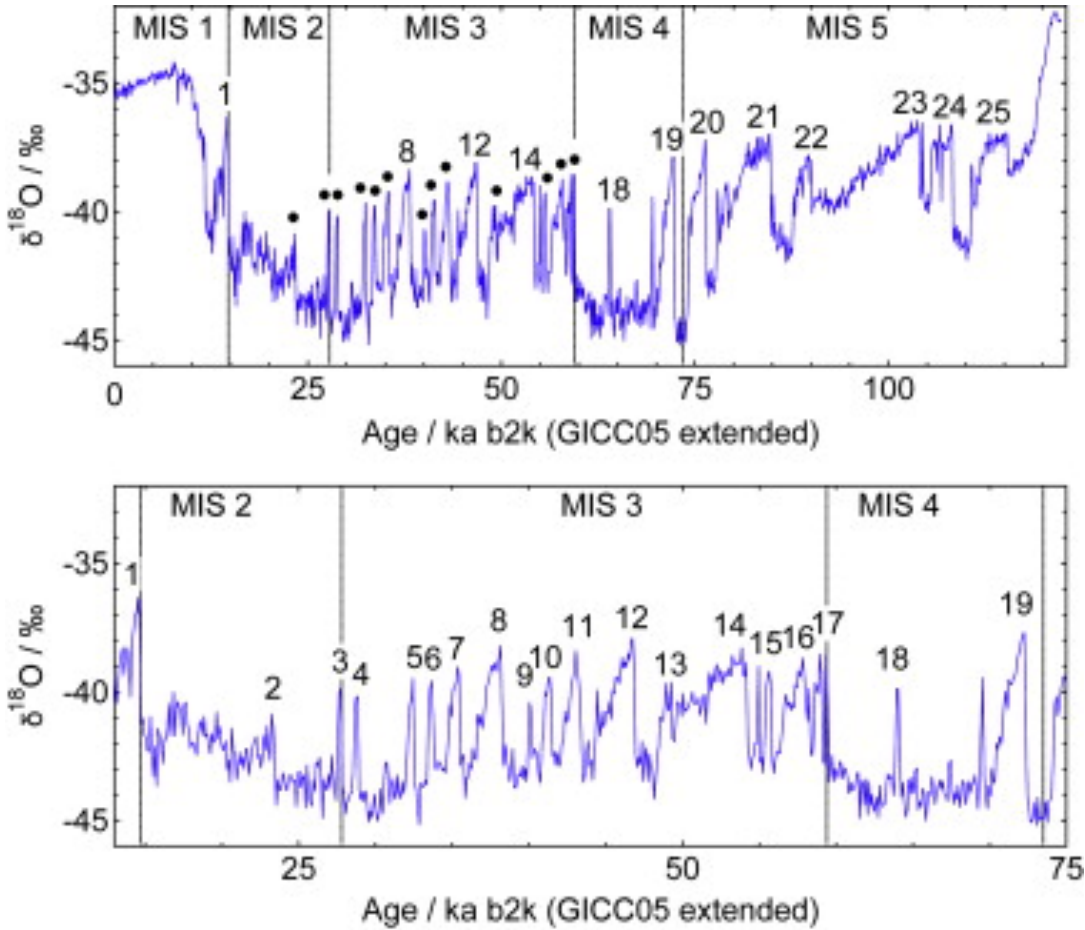


Figure 1: Numbering of D-O oscillations from MIS 1-5 (top) and focusing on MIS 2-4 (bottom) (Wolff et al., 2010).

2.3 The Atlantic Meridional Overturning Circulation

D-O oscillations are heavily associated with changes in the AMOC. This idea of the AMOC being responsible for these rapid climate changes was popularized by Broeker et al. (1985), who proposed that the warm interstadials and cold stadials corresponded with two different modes of oceanic circulation. Consequently, a brief background on the AMOC will be provided. The AMOC is part of the global thermohaline circulation, illustrated in Figure 2 (Kuhlbrodt et al., 2007). There are four main branches of the AMOC that form its circulation pattern, as also illustrated in Figure 2. At high northern latitudes, the cooling of surface water causes it to become denser and sink down to depths, resulting in the formation of North Atlantic Deep Water (NADW). This cold water then flows southwards in deep currents, eventually upwelling back up to the surface. These upwelling processes bring water from depth to the upper layers of the Atlantic. This lighter water is then carried by surface processes to high northern

latitudes where NADW formation occurs, thus forming a circulation loop (Kuhlbrodt et al., 2007). These four branches then form two overturning cells in the AMOC: a dominant “upper” cell that includes the formation of NADW which flows southward at 1,500-4,500 m in depth, and a “deep” cell of Antarctic Bottom Water (AABW) that flows northwards at depths below 4,500 m and rises to join the NADW flowing south (Kuhlbrodt et al., 2007; Dalworth et al., 2008). These two cells in their present-day configuration are outlined in the “warm” mode in Figure 3 (Rahmstorf, 2002). The upper cell is responsible for carrying heat to higher latitudes, which consequently results in it acting as a heat source for much of Europe, especially during the winters (Buckley and Marshall, 2015; Broecker and Denton, 1989).

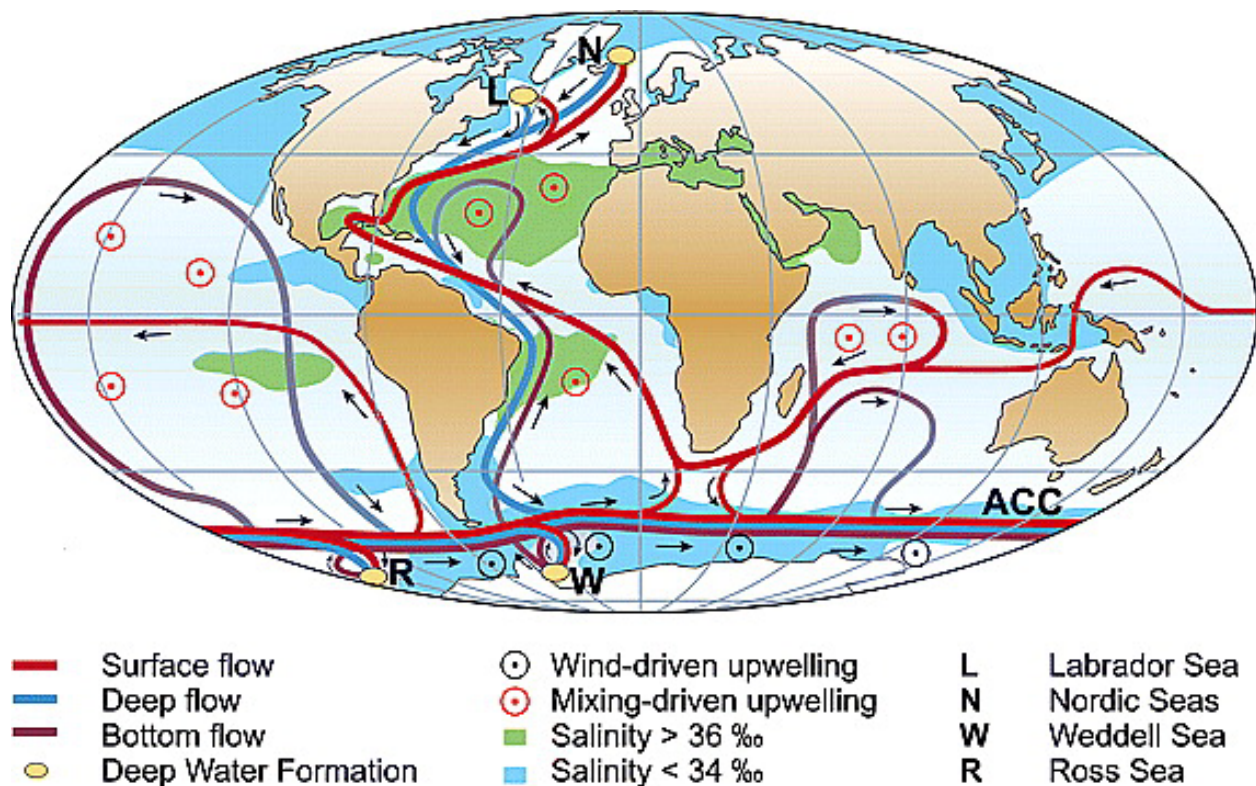


Figure 2: Simplified sketch of global overturning circulation (Kuhlbrodt et al., 2007). Seen is the AMOC, which consists of the upwelling processes in the Atlantic and the deep-water formation processes in the North Atlantic, which are connected by a southward deep flow and a northward surface flow.

It is therefore quite evident that the climate in the Northern Hemisphere can be strongly influenced by the AMOC. Rooth (1982) originally posited that abrupt climate change could stem from a weakening of the AMOC in an effort to explain a specific return to cold conditions in MIS1 called the Younger Dryas. Broecker et al. (1985) subsequently expanded this theory to

cover the observations of oscillations in MIS3 that would later be dubbed D-O oscillations. Broecker et al. (1985) continued with Oeschger's proposal of two modes of climate by suggesting how one mode corresponds to a situation when NADW formation is strong while the other corresponds to weak NADW formation. In this proposed mechanism, the "strong" mode corresponds to the present-day climate along with other warm periods, whereas the "weak" mode corresponds to glacial times (Broecker et al., 1985). It is then proposed that the two modes switch back and forth; when the weak mode is present, the stoppage of the AMOC causes a warming in Antarctic waters, which in turn reduces the density of deep water which favours NADW formation (Blunier et al., 1998). When NADW starts forming, the circulation switches back on into the strong mode, and causes ice rafting events that will start cooling the Southern Hemisphere (Blunier et al., 1998). Consequently, on top of these two modes, Broecker (1998) describes a "bipolar seesaw" model, in which the Northern and Southern Hemispheres were in antiphase in terms of response to a switching of modes. The exact phasing between the two hemispheres is still debated as various model results have shown the hemispheres to be in-phase, time lagged, or antiphase. For example, the model from Knutti et al. (2004) supports a hemispheric antiphase pattern whereas the model from Peltier et al. (2020) shows an in-phase relationship between the hemispheres. Additional differences between these models will be discussed in a later section.

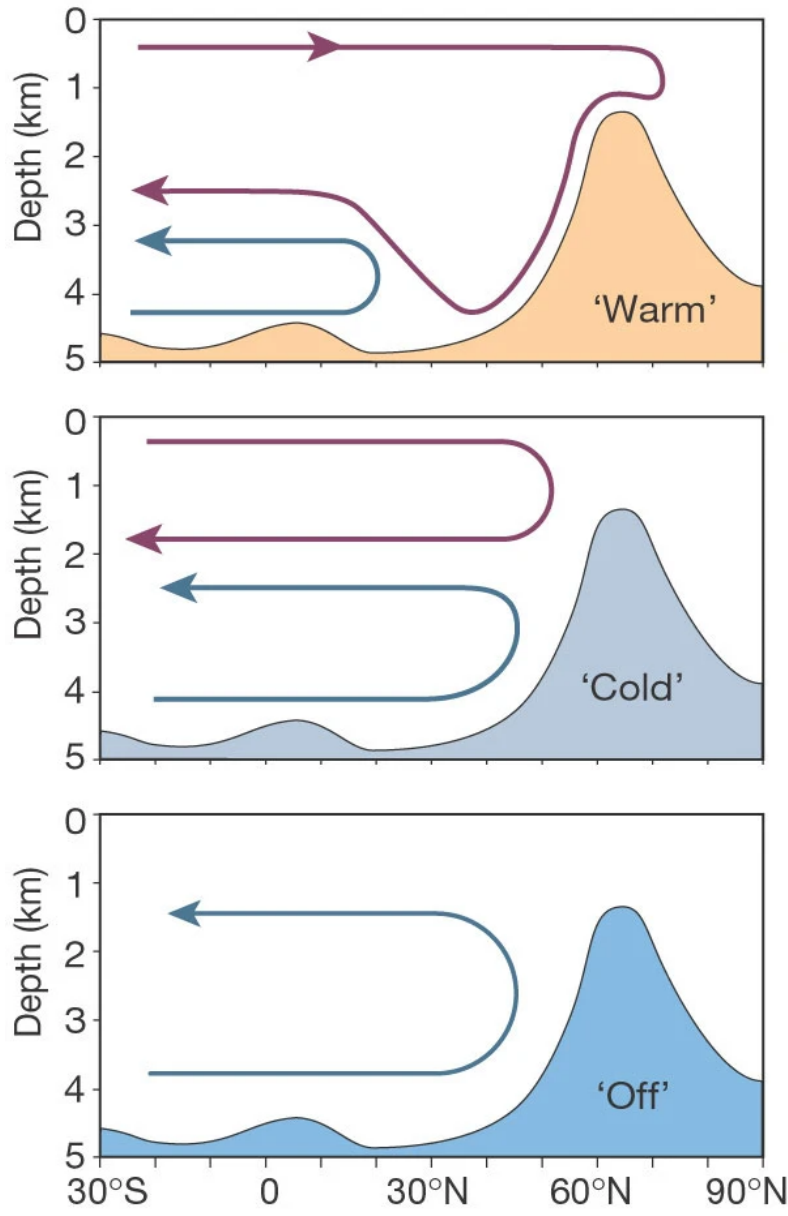


Figure 3: Different modes of the AMOC (Rahmstorf, 2002). This includes (from top to bottom) the modes that correspond with interstadials, D-O stadials, and Heinrich stadials.

Currently, it appears that there are actually three main modes for the AMOC: the modern “warm” mode, a glacial “cool” mode, and a “off” mode that could be associated with Heinrich events (Alley and Clark, 1999; Ganopolski and Rahmstorf, 2001). A simplified illustration of these modes can be found in Figure 3. The model done by Ganopolski and Rahmstorf (2001) is also a significant model to make note of and will be discussed further in the review amongst other models. Strong physical evidence for changes in the AMOC were presented by McManus et al. (2004), who utilized ^{231}Pa and ^{230}Th ratios in a sediment core taken from the subtropical

North Atlantic as a proxy for AMOC strength. These two isotopes form when ^{235}U and ^{234}U isotopes that are dissolved in the seawater radioactively decay, and their different residence times imply different removal rates from the subtropics by the AMOC (McManus et al., 2004). This ^{231}Pa and ^{230}Th ratio profile captured changes in AMOC strength that followed temperature changes reflected in $\delta^{18}\text{O}$ profiles taken from planktonic foraminifera in the core (McManus et al., 2004). These profiles in turn illustrate the changes in climate associated with the Last Glacial Maximum, Heinrich event 1, the Bølling-Allerød warm period, and the Younger Dryas Cold period (McManus et al., 2004). In all, the AMOC is a significant factor in global climate, and changes in its various modes can be linked to the D-O oscillations observed through various paleoclimate proxies. The next portion of the report will focus on detailing D-O oscillations through their various components, namely interstadials and stadials, while also touching on Heinrich events, which are closely related to D-O oscillations.

2.4 Description of Interstadials

The start of an interstadial, the warm period in a D-O oscillation, is characterized by a sudden, drastic warming on a decadal scale. After this warming, interstadials can last for 500 to 2000 years, and seem to be irregularly occurring (Johnsen et al., 1992). Initially using the linear relationship between $\delta^{18}\text{O}$ and temperature, Johnsen et al. estimated a temperature difference of about 7°C between the warm interstadial and the cold stadial (Johnsen et al., 1992). The jump to an interstadial was also very drastic, with these temperatures increasing on a decadal scale; similar abrupt jumps can be seen at the termination of the Younger Dryas (seen in MIS1 in Figure 1), where a 7°C increase was observed to have occurred in only a 50-year span (Dansgaard et al., 1989). Later techniques involving the deconvolution of borehole temperature profiles showed that this increase was likely more drastic (Johnsen et al., 1995). Consequently, more recent studies using $\delta^{15}\text{N}$ as a temperature proxy and additional adjustments based off firn densification and heat diffusion show temperature swings ranging between 5°C to 16.5°C (averaging to $12\pm2.6^\circ\text{C}$) for the D-O oscillations shown in Figure 1 (Kindler et al., 2014). The D-O interstadials are highlighted by the peaks in $\delta^{18}\text{O}$ in the figure. Looking at ^{231}Pa and ^{230}Th ratios from cores taken from the North Atlantic and comparing them with temperature proxy data, there is also a clear relationship between the strengthening of the AMOC and a warming of temperatures during D-O interstadials (Henry et al., 2016). This strong AMOC is consistent with

its current “warm” mode, and consequently climates in the Northern Hemisphere during interstadials are also relatively warm (Fletcher et al., 2010). This can be observed through warmer temperatures and also a reduction in Norwegian Sea sea-ice cover (Sadatzki et al., 2019). Furthermore, this warmer Northern Hemisphere encouraged tropical wetland formation, which can be seen in the form of enhanced methane signals in ice core records, which also implies a northward shift of the Intertropical Convergence Zone (ITCZ) (Tzedakis et al., 2009). This northward shift of the ITCZ indicates a warmer and wetter Northern Hemisphere. In all, during interstadials, the AMOC is strong and consequently, the climate is more temperate and similar to that of the present.

2.5 Description of D-O stadials

D-O stadials are the cold periods associated with D-O oscillations. After the rapid transition to an interstadial in the Greenland ice cores, a gradual cooling lasts between 500 to over 2000 years, followed by a faster cooling on a decadal scale that causes the drop into stadial conditions (Johnsen et al., 1995; Wolff et al., 2010). Outside of the temperature fluctuations in the Greenland ice cores, a general cooling trend can be observed throughout areas of the Northern Hemisphere during the stadials (Fletcher et al., 2010). These cold temperature trends resulted in an increase in Norwegian Sea sea-ice cover (Tzedakis et al., 2009). While interstadials are characterized by warmer and wetter conditions in the north, stadials are characterized by colder and dryer conditions. In regard to the AMOC strength, it is observed to be weaker during D-O stadials (Henry et al., 2016). This weakening of the AMOC is characterized by a gradual warming in the southern hemisphere (EPICA Community Members, 2006). This warming in southern latitudes during the stadials adheres to Broecker’s proposed “bipolar see-saw” model (Broecker, 1998). This therefore leads to a southward shift of the ITCZ, which implies wetter southern tropics (Schneider et al., 2014). It should be noted however that the peak air temperatures of both hemispheres appear to be in phase, though with a potential on-average time lag (WAIS, 2015). This can be seen in Figure 4, where although the northern temperatures are cooling at the start of the stadial and the southern temperatures are rising, the peak temperatures are generally in phase. Overall, D-O stadials predictably exhibit the opposite behaviour of interstadials to form the full D-O oscillation.

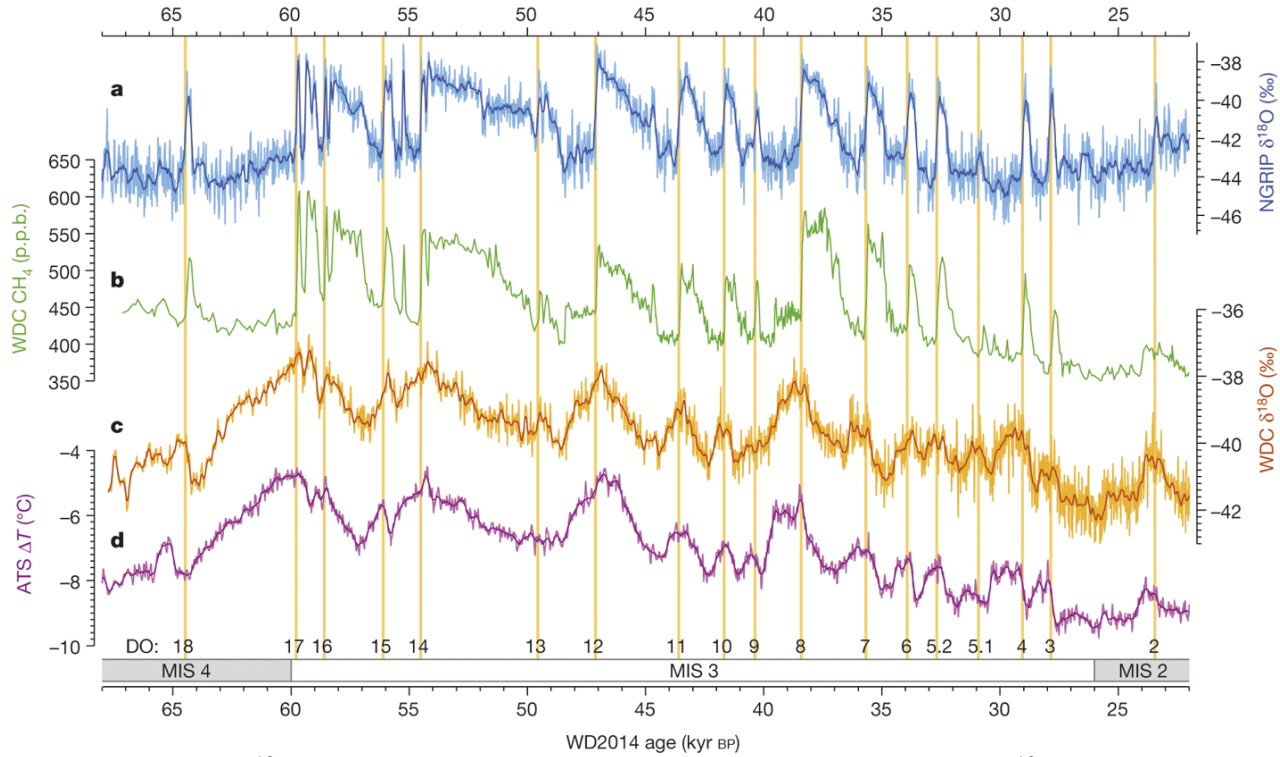


Figure 4: NGRIP $\delta^{18}\text{O}$ (a), WAIS divide ice core (WDC) methane (b), WDC $\delta^{18}\text{O}$ (c), and Antarctic Temperature Stack (ATS) relative to present day (d) records (WAIS, 2015).

2.6 Description of Heinrich events

Heinrich events show up in the Greenland ice cores in a similar fashion to D-O stadials – they share similar amplitudes in terms of $\delta^{18}\text{O}$ measurements (Kindler et al., 2014). However, the main factor differentiating Heinrich stadials from D-O stadials is that they result in high levels of ice-raftered debris (IRD), which corresponds to a large number of icebergs being discharged (Heinrich, 1988). This IRD can be found in an area known as the Ruddiman belt stretching across the North Atlantic, illustrated in Figure 5. Bond and Lotti (1995) noted that smaller ice-calving events still occurred during D-O stadials in 2000 to 3000-year intervals, which is a higher frequency than the 7000-10,000-year period for Heinrich events. Heinrich events during the last glacial cycle are highlighted amongst the rest of the D-O oscillations in Figure 6 (Peltier and Vettoretti, 2014). From this figure it appears that the Heinrich events kick off a set of D-O oscillations, with the subsequent oscillations decreasing in amplitude and period. This pattern is also known as a Bond cycle, in which a Heinrich event is followed by D-O oscillations of decreasing amplitude (Kageyama et al., 2010). Consequently, it has been proposed that Heinrich events trigger D-O oscillations (Timmerman et al., 2003). It also appears that Henrich events

have more extreme temperatures when compared to their D-O stadial counterparts and last longer (Kinder et al., 2014). Figure 7 shows the difference between a D-O stadial and a Heinrich event, and it can be seen that although both cause colder, drier conditions over the North Atlantic and Europe and warmer, wetter conditions in the South Atlantic, the changes induced by a Heinrich event are more drastic (Menziel et al., 2020). This, along with an even weaker AMOC than D-O stadials, suggests that Heinrich events represent the third mode of the AMOC, the “off” mode (Henry et al., 2016). This contrasts with the “cold” mode illustrated in Figure 3 associated with a D-O stadial. Overall, the effects of Heinrich events are comparable to stronger versions of D-O stadials. Furthermore, these ice-rafting events offer a potential trigger for subsequent oscillations, which leads into the next section of the review which addresses the mechanisms behind D-O oscillations.

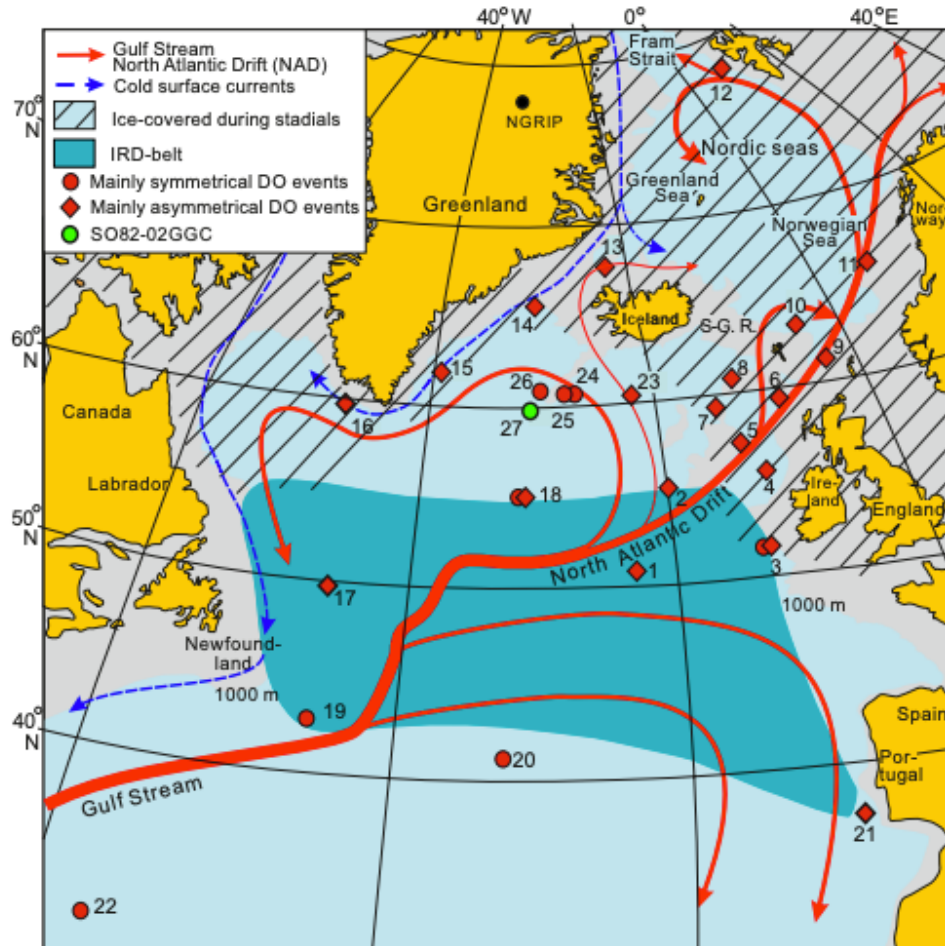


Figure 5: Map illustrating IRD belt (known as the Ruddiman belt), along with locations of various palaeoceanographic records (Rasmussen et al., 2016)

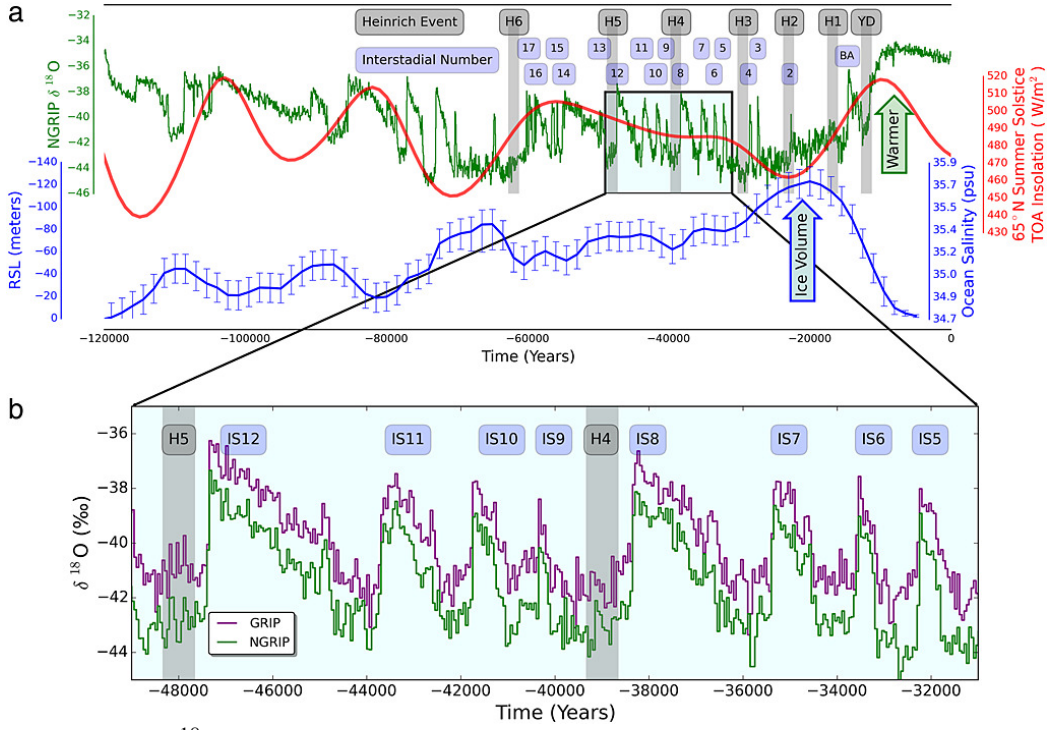


Figure 6: a) NGRIP $\delta^{18}\text{O}$ (green), insolation at 65°N (red), and relative sea level (blue) over the last glacial cycle. b) NGRIP (green) and GRIP (purple) $\delta^{18}\text{O}$ profiles for a subsection of MIS3 (Peltier and Vettoretti, 2014).

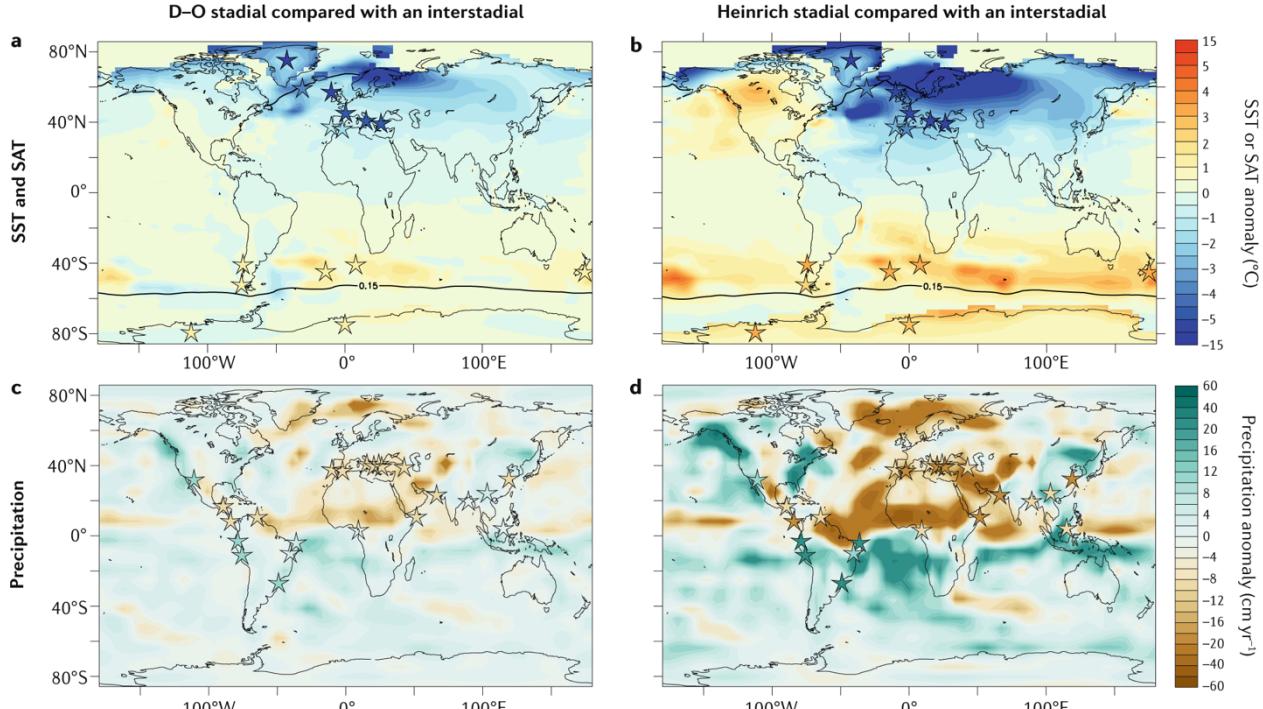


Figure 7: Simulation results from Men viel et al. (2014) plotted to illustrate sea surface and surface-air temperature (SST and SAT) anomalies for D-O stadials (a) and Heinrich stadials (b), along with precipitation anomalies for D-O stadials (c) and Heinrich stadials (d) (Men viel et al., 2020).

2.7 Mechanisms

It is clear that variabilities in the AMOC play an important role in D-O oscillations, and an explanation is needed for what factors cause those variabilities. Within models, there are primarily two methods of simulating D-O oscillations, either through freshwater forcing or through “spontaneous” self-sustained oscillations caused by internal instabilities (Li and Born, 2019). Due to the prevalence of the ocean circulation mechanisms popularized by Broecker et al., some studies still necessitate the requirement for a freshwater forcing element in triggering D-O oscillations. Broecker et al. (1990) proposed that D-O oscillations depended on a “salt oscillator” in the Atlantic. Such a “salt oscillator” works in the following fashion: starting with an “off” mode, the salt in the North Atlantic builds up due to vapor loss and ice sheet growth, and hence the water grows denser (Broecker et al., 1990). Once this density reaches a threshold, the conveyor switches to an “on” mode (or a warm mode as described earlier). When the conveyor is on, the salt content (and therefore the density) of the North Atlantic would gradually decrease due to an increased salt export and meltwater input, eventually switching the circulation back to the “off” mode (Broecker et al., 1990). A central assumption made by Broecker et al. (1990) is that to prevent the conveyor from self-stabilizing in the “on” mode, additional meltwater input is required to dilute surface waters in the North Atlantic; the stoppage of this meltwater input in the “off” mode is also what counters the stabilization of that mode. Alley et al. (2001) hypothesize that this freshwater forcing can be quite weak as it would be significantly amplified through stochastic resonance by combining it with “noise” from ice sheet-related events. Consequently, due to the apparent need of a meltwater factor, many models utilize a freshwater perturbation in triggering the overturning changes necessary to cause a D-O oscillation (Ganopolski and Rahmstorf, 2001; Knutti et al., 2004). These models are examined further in the modelling section of the background.

Although there is evidence of freshening in the North Atlantic during D-O stadials, it is not certain if it is enough to disrupt the AMOC (Menviel et al., 2020). Furthermore, there is a potential that the observed iceberg discharges (and source of fresh water) occur after the North Atlantic cooling starts, meaning that they cannot be the freshwater trigger for D-O oscillations (Barker et al., 2015). Likewise, there are modelling studies that question the significance of freshwater forcing as a trigger for D-O oscillations stemming from box model-based analyses

(e.g., Peltier and Sakai, 2001). In a series of models by Sakai and Peltier, they examine how the thermohaline circulation could potentially “fibrillate” without the presence of an explicit freshwater forcing (Peltier and Sakai, 2001). New modelling-based studies suggest now that D-O oscillations could be a “spontaneous” climate oscillation (e.g., Drijfhout et al., 2013; Peltier and Vettoretti, 2014). In the Peltier and Vettoretti (2014) model, it is shown that the D-O oscillations are indeed a “salt oscillator”, but they are in the form of a relaxation oscillator. After an initial kick by a pseudo-Heinrich event, oscillations are driven by salinity and sea-ice processes and do not require additional freshwater forcing (Peltier and Vettoretti, 2014). As to be discussed later, this model has its limitations, and consequently there is still research that can be done to understand the mechanisms behind D-O oscillations. On the other hand, the Drijfhout et al. (2013) model utilized stochastic atmospheric forcing. Other models seem to relate changes in carbon dioxide levels to AMOC changes (Klockmann et al., 2018, Zhang et al, 2014). However, it seems that currently there is no strong evidence of significant changes in CO₂ concentration during D-O stadials, and that an increase in CO₂ concentration is only observed with Heinrich stadials (Menziel et al., 2020). A detailed diagram and explanation on the possible mechanisms behind the D-O oscillations can be seen in Figure 8 (Menziel et al., 2020). Identifying the triggers for Heinrich events is a separate investigation that is not included in the scope of the background. The Peltier and Vettoretti (2014) model, amongst others, are discussed further after a brief background on climate modelling.

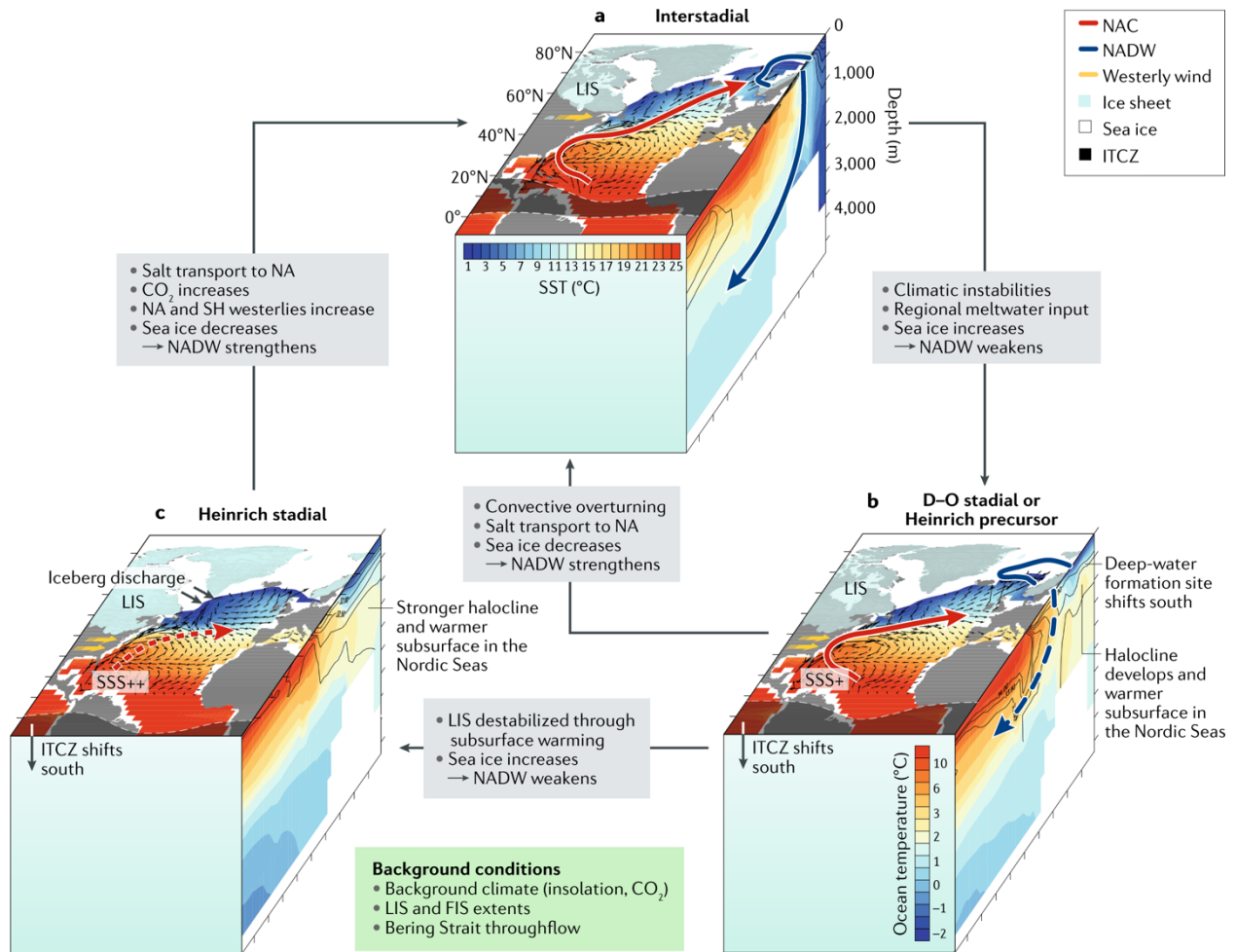


Figure 8: Proposed mechanisms for D-O oscillations by Menviel et al. (2020). These mechanisms connect the schematics for interstadial (a), D-O stadial (b), and Heinrich stadial conditions.

3. Background on Climate Modelling

3.1 A History of Climate Modelling

As often discussed, climate models have proven to be a great method in gaining an understanding of past climates. This section will provide a brief history on how climate models are set up and run, along with recent D-O oscillation modelling efforts. The crux of climate modelling lies in having equations that can properly represent the climate system. Some of the earliest models of climate were physical models such as rotating dishpans that could demonstrate fluid motions, but ultimately had very limited capabilities (Edwards, 2010). The earliest mathematical models were energy balance models (EBMs), and as their names suggest, consisted of equations balancing the incoming solar energy and the outgoing energy in the form of longwave emission (Edwards, 2010). One early example is the model developed by Mikhail Budyko, who used it to conclude that the climate was very sensitive to small fluctuations and that small changes in the atmosphere could have caused the shifts towards glaciation during the ice ages (Budyko, 1969). Simple, one-dimensional energy balance models were utilized to estimate the Earth's average atmospheric vertical temperature profile, whereas more complicated two-dimensional EBMs which included poleward diffusion of heat and land-sea contrasts were used to gain insights into the zeroth-order global distribution of temperatures. Radiative-convective models, using equations representing energy transfer between atmospheric layers, also modelled the same vertical and meridional profiles (Edwards, 2010). For more modern models, additional mathematical equations are necessary to properly represent climate dynamics, and thus the models become quite complex and require the aid of computers.

The “primitive equations” used by modern General Circulation Models (GCMs) were developed in the early 1900s by Vilhelm Bjerknes, though computational requirements resulted in the first computerized GCMs appearing in the 1950s (Edwards, 2010). On top of the thermodynamic energy balance equation, Bjerknes included equations describing the conservation of mass and momentum within a system to form his “primitive equations” (Bjerknes, 1910). With the advent of computers and better computational methods, these primitive equations were utilized to model atmospheric motion on a regional or even global scale. This was done by breaking down the globe into grid components and utilizing those equations to calculate exchanges between grid components (Edwards, 2010). Modern GCMs still

follow this logic, using these primitive equations for large-scale fluid motions while simulating other processes such as cloud formation with different models. As more physical processes get added, these models become more complex, and require greater computational power for viable resolutions and timescales. A simple illustration of the increase in complexity of the processes incorporated into models can be found in Figure 9. From there it can be seen that over time, ocean and land processes were joined with atmospheric processes, and those processes were in turn explored in more detail through the modelling of factors such as vegetation or aerosols (Le Treut et al., 2007). Likewise, the resolution of climate models has improved drastically over time, as shown in Figure 10. This also includes an improvement of the vertical resolution (not shown in Figure 10), where earlier models only had a single-slab ocean and ten atmospheric layers compared to models at the time of IPCC's fourth assessment report (AR4) which have about thirty levels in both the atmosphere and the ocean (Le Treut et al., 2007). This evolution of models can be seen in the progression of historical models that led to the model used by this current project, the National Center for Atmospheric Research (NCAR) Community Climate System Model 4 (CCSM4).

The World in Global Climate Models

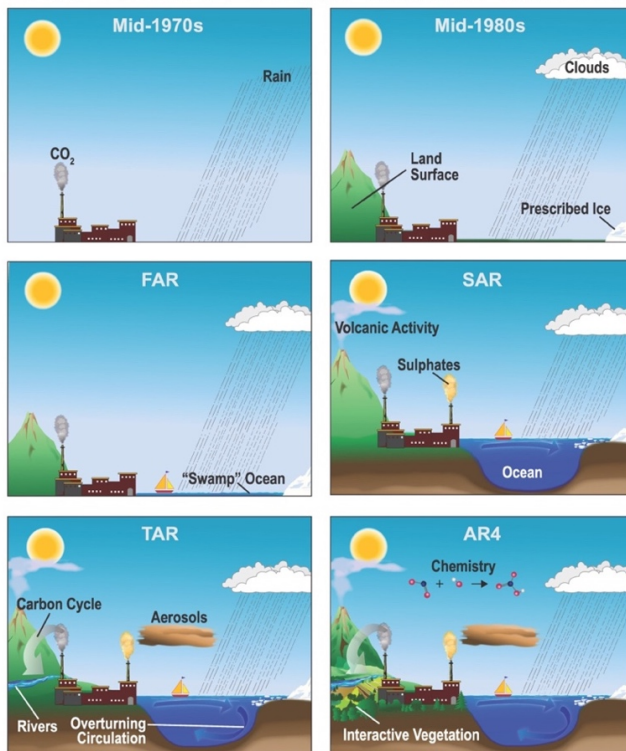


Figure 9: The increase in complexity of climate models up to the release of IPCC AR4 (Le Treut et al., 2007)

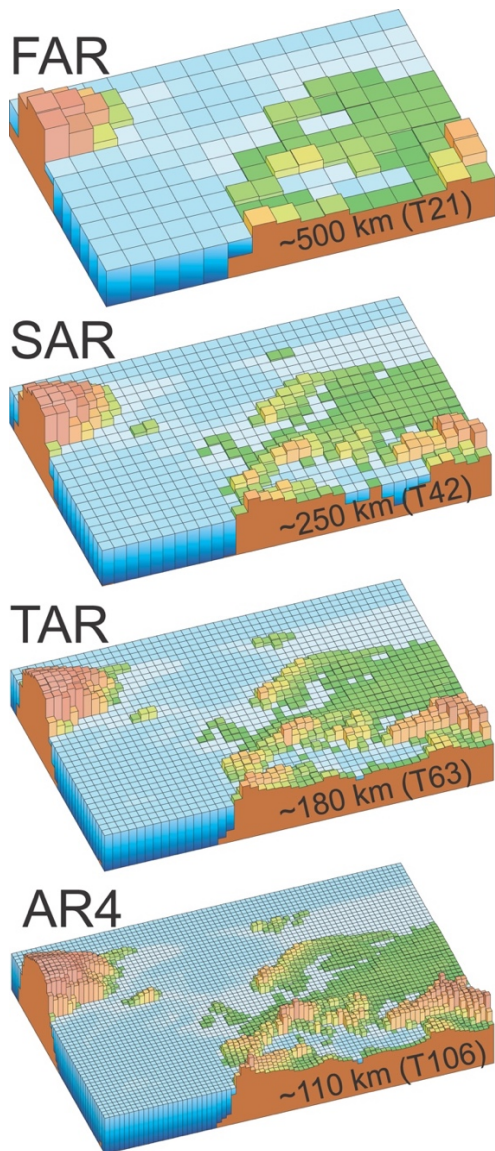


Figure 10: The increase in resolution of climate models up to the release of IPCC AR4 (Le Treut et al., 2007)

In the historical development of climate models, there are some important ones to note, as their setup/logic can still be seen in modern models. One significant step was made by Norman Phillips, who created a two-level geostrophic model that demonstrated realistic atmospheric flow patterns (Phillips, 1956). Phillips' model was significant as it was built directly upon the primitive equations, thus emphasizing the importance of starting with the primary physics (Phillips, 1956; Edwards, 2010). Phillips then worked with Joseph Smagorinsky among others to develop models, and Smagorinsky subsequently brought on Syukuro Manabe and Kirk Bryan to work at the General Circulation Research Station created by the US Weather Bureau

(Smagorinsky, 1958; Edwards, 2010). Manabe and Bryan then developed a very significant model by coupling the ocean and the atmosphere and allowing them to interact with one another (Manabe and Bryan, 1969). Although the ocean-continent configuration was quite simple and idealized, the modelling by Manabe and Bryan is significant because of its coupling of systems, which can be seen throughout modern models. Finally, Kasahara and Washington at the National Center for Atmospheric research (NCAR) made significant developments by creating early spectral models, which analyzed horizontal motion in a wave space and subsequently transformed back into a grid space representation (Edwards, 2010). Spectral models proved to be more efficient than earlier grid-based, finite-difference methods, which tended to have difficulty performing calculations for higher latitudes along with representing wave motion on a sphere (Edwards, 2010). NCAR’s Community Climate Model (CCM) series are spectral models and are the forerunners to the CCSM4 model used by this project.

3.2 Modelling D-O Oscillations

Outside of the usage of the NCAR CCSM4 model for D-O oscillations, there exist other models that have simulated these oscillations. A significant one is CLIMBER-2, an Earth System Model of Intermediate Complexity (EMIC), which was utilized by Ganopolski and Rahmstorf (2001). The intermediate complexity refers to both a coarser resolution, along with simpler models for various processes. With the CLIMBER-2 EMIC, the spatial resolution is quite coarse (2.5° , with 20 vertical levels for the ocean model), and as a result it is used for long-term climate simulations. Nevertheless, it is a coupled climate model and has modules that describe atmospheric, oceanic, sea ice, land surface, terrestrial vegetation, and carbon cycle processes (Petoukhov et al., 2000). With this model, Ganoopolski and Rahmstorf (2001) find that only one mode of circulation is stable: the “cold” mode where there is less deep-water formation; the “warm” mode is found to be marginally unstable, into which temporary transitions from the “cold” mode can occur. They introduce a small freshwater forcing of unknown origin to trigger this transition, finding that a periodic (period of 1,500 years) 0.03 Sv ($10^6 \text{ m}^3/\text{s}$) of freshwater forcing to the Atlantic was enough to trigger D-O-like oscillations (Ganopolski and Rahmstorf, 2001). However, this forcing is of unknown origin, and ice cores do not seem to provide evidence for such a period of forcing as noted by Peltier et al. (2020). Peltier et al. (2020) also refer to another EMIC of significance, and that is the ECBILT-CLIO model used by Knutti et al.

(2004) which also used freshwater forcing. This model has an oceanic resolution of 3° and 20 levels and introduces a freshwater forcing of around 0.5 Sv for the duration of a Heinrich event, and they do this for every D-O oscillation, not just the Heinrich events (Knutti et al., 2004). During this forcing, the sea level increases up to 15 m, which is much higher than previously calculated (Hemming, 2004). They also observed much shorter signaling times than ones calculated for the “bipolar seesaw” by Stocker and Johnson in 2003 while also acknowledging that the “pacemaker” behind these oscillations was undetermined (Knutti et al., 2004). Menviel et al. (2014) likewise had freshwater forcing in their LOVECLIM (also with an oceanic resolution of 3° and 20 levels) modelling efforts and concluded that the AMOC variations driven by freshwater forcing caused D-O oscillations, though it now remains uncertain (Menviel et al., 2020). Evidently, there are still many unanswered questions with these EMICS, namely the uncertainties with freshwater forcing. The model of use in this project, the UofT-CCSM4 model, is of interest as it does not require freshwater forcing to produce these oscillations and will as a result be the focus of the next section.

3.3 The UofT-CCSM4 Model

UofT-CCSM4 (Peltier and Vettoretti, 2014) is a specific configuration of the NCAR CCSM4 (Community Climate System Model 4) model (Gent et al., 2011). This model with a nominal resolution of 1° consists of sub-models that simulate the atmosphere, ocean, land, and sea-ice and which are joined via a coupler (Gent et al., 2011). A summary of each component is provided in Table 1. The modifications to the University of Toronto version of CCSM4 are limited to the ocean component and are focused on changes to the diapycnal and related momentum diffusivities; this is due to the CCSM4 model utilizing a modern tidal regime, with which the turbulent diffusivity is directly tied. UofT-CCSM4 also differs from the public release of the model in that the overflow parameterization was eliminated because it had been tuned to modern bathymetry (Peltier and Vettoretti, 2014).

The D-O simulations performed with this model used glacial maximum boundary conditions from the ICE-6G (VM5a) model of Peltier et al. (2015) and Argus et al. (2014). In the course of the spin up of the model, upon crossing a thermal threshold, the AMOC experiences a sharp reduction in strength that kicks off the D-O oscillations (Peltier and Vettoretti, 2014). This

sharp reduction in AMOC strength is referred to as a pseudo-Heinrich event (labelled “H” in Figure 11) and is similar to that which would be achieved if there were a real Heinrich event. These oscillations are the only instance where D-O oscillations were created in a high-resolution climate model under glacial boundary conditions.

Table 1: Components of CCSM4 utilized in UofT-CCSM4 (Peltier and Vettoretti, 2014)

Component	Model	Details
Atmosphere	Community Atmosphere Model version 4 (CAM4)	0.9° x 1.25° finite volume resolution, 26 levels
Land Surface	Community Land Model (CLM4)	Same resolution as atmosphere, includes carbon-nitrogen biogeochemistry model
Ocean	Parallel Ocean Program version 2 (POP2)	~1° varying resolution (~0.25° in tropics), 60 levels
Sea Ice	Community Ice Code version 4 (CICE4)	Same orthogonal grid as oceans

From the Peltier and Vettoretti (2014) results, it was proposed that the abrupt transition in a D-O oscillation from stadial to interstadial conditions is accompanied by the opening of a large polynya (large opening in sea ice) in the North Atlantic sea ice cover (Vettoretti and Peltier, 2016). The resulting resumption of exchange of fluxes between the atmosphere and the ocean aided the erosion of the vertical salinity gradient that had prevented convective destabilization of the water column, which stems from an increase of salinity closer to the ocean’s surface beneath the sea ice (Vettoretti and Peltier, 2018). On the other hand, the more gradual transition from interstadial to stadial is characterized by the flux of sea ice into the North Atlantic which restratifies the ocean surface and consequently reduces NADW formation and returns the climate to stadial conditions (Vettoretti and Peltier, 2018). As emphasized throughout this report, these processes did not depend upon the action of external freshwater forcing, which were critical to all earlier efforts to produce DO-like oscillations. Rather, it was later shown that the AMOC period was very closely correlated with the diapycnal diffusivity parameter, which controls the characteristic opening/closing of the polynya mentioned earlier (Peltier et al., 2020). The results from this model, with all its components and also without a double diffusion component, can be seen in Figure 11. Figure 11 also plots simulated temperatures at ice core sites in Antarctica and Greenland, from which the phasing between the two hemispheres can be seen.

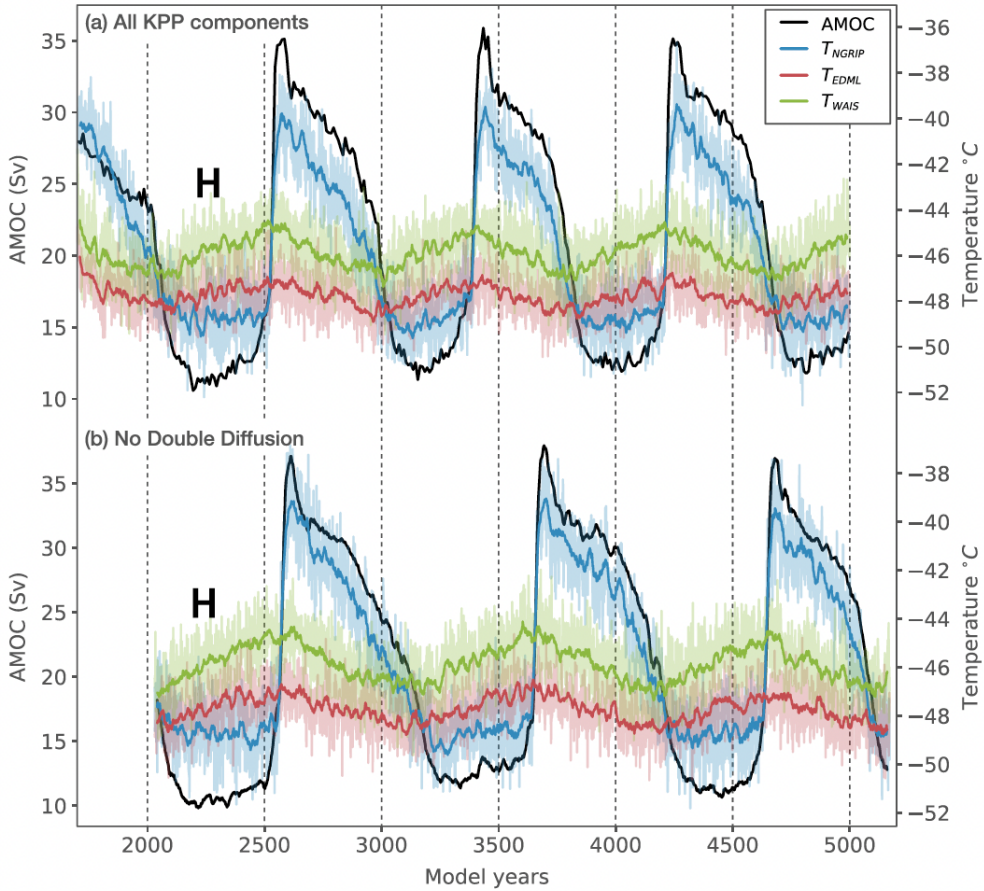


Figure 11: Simulated AMOC strength (black) compared to simulated temperature fluctuations in the NGRIP (blue), EDML (red), and WAIS (green) ice cores (Peltier et al., 2020)

3.4 Experiment opportunity

As noted in the introduction, the results of Peltier et al. show that the peak warming periods for both hemispheres are exactly in-phase (Figure 11; Peltier et al., 2020). This contrasts with other studies that have estimated a time lag, notably one done by members of the West Antarctic Ice Sheet Divide project, which posits that Greenland events lead Antarctic events by 218 ± 92 years (WAIS, 2015). The reasons behind this divergence could possibly be explained by the neglect of continental freshwater exchange in the existing D-O simulations; the first oscillation triggered by the Heinrich event should be in-phase, but subsequent cycles may have a shift stemming from a freshwater flux in the form of meltwater from grounded ice on the continents. Another reason, as noted by Peltier et al. (2020), could be that the WAIS study averaged multiple D-O oscillations, which might have resulted in a questionable time lag as each cycle has different time scales and proximities to the Heinrich event that kicked off a train of

oscillations. Another important observation to note is that the oscillations captured by Peltier et al. (2020) have an “infinite-Q”, meaning that they are uniform in period and amplitude. This is not the case in the ice core data, where the subsequent pulses after the first have decreasing periods and amplitudes, or a “finite-Q”. There is a proposal that additional freshwater forcing could shape the oscillations, so they have such a “finite-Q”. This forms the basis of this thesis project, which adds additional freshwater forcing to the UofT-CCSM4 model to investigate its impacts.

Comparisons between freshwater forced and unforced models have been done previously. One such example is by Brown and Galbraith (2016), who utilized the CM2Mc model for their analysis (Galbraith et al., 2011). They however utilized 0.2 Sv of freshwater hosing applied for 1000 years, and their results consequently had hosed events evoking Heinrich stadials whereas their unhosed events resemble D-O stadials (Brown and Galbraith, 2016). This specific project is different than that of Brown and Galbraith’s in that it also examines hosing during the transition from stadial to interstadial, which is a much shorter time than the 1000 years utilized by Brown and Galbraith. Zhang et al. (2014) also inspect the impact of freshwater forcing, using the COSMOS model (ECHAM5 atmosphere model, JSBACH land surface model, MPI-OM ocean model; Zhang et al. 2013), and note that it can trigger significant responses in ocean circulation. However, they only added 0.02 Sv perturbations during the strong or weak AMOC state, and not during the transitions as this project also did.

4. Methods

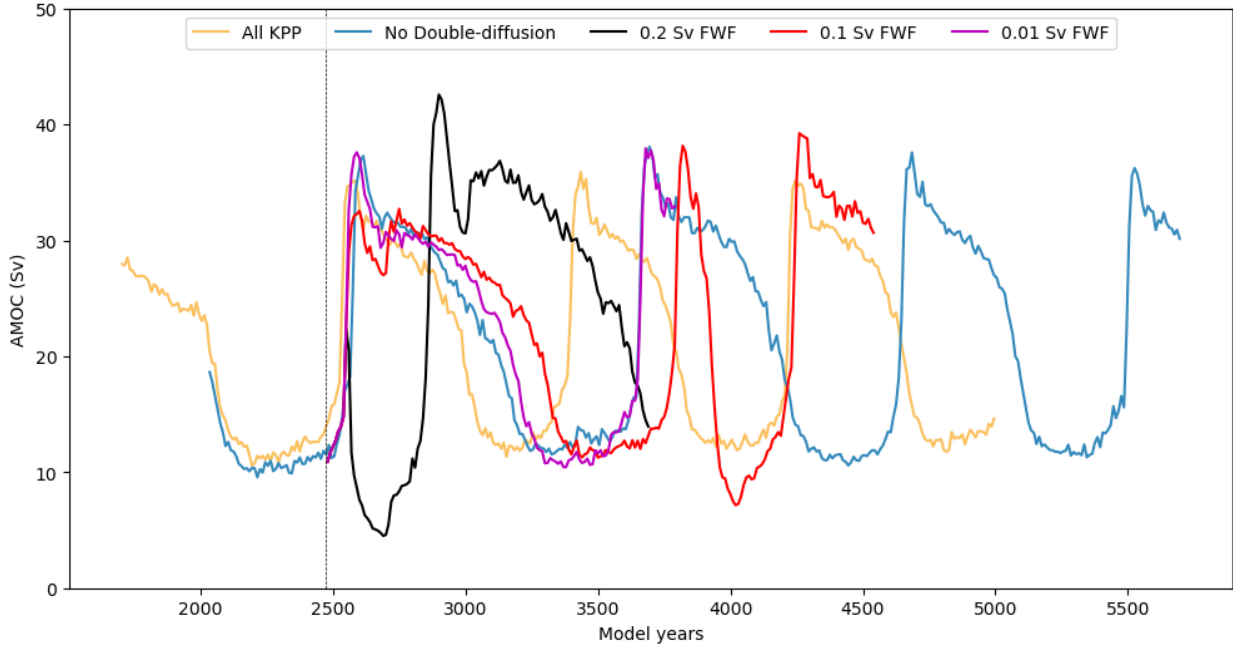


Figure 12: Comparison of the AMOC timeseries collection of all the simulations done for this project (0.2 Sv, 0.1 Sv, and 0.01 Sv of freshwater forcing) compared with the “All KPP” and “No double-diffusion” runs from Peltier et al. (2020). This shows how all the runs branch off at model year 2475 (marked by the dashed line), and vary differently based off forcing parameters, which are detailed in further figures.

Over the course of this project, three models were set up under the guidance of Dr. Deepak Chandan and were run on Niagara, a supercomputer hosted by SciNet at the University of Toronto. Appendix A contains additional details about SciNet, and Appendix B includes a detailed description of the setup, running, and processing of these models. All three models were branched from the noDD (no double-diffusion) simulation of Peltier et al. (2020) at model year 2475, which is when the noDD model is just beginning to transition from the stadial to the interstadial stage (Figure 12). The new models are named DO.nodd.fwf.v1, DO.nodd.fwf.v2, and DO.nodd.fwf.v3 (henceforth referred to simply as v1, v2, and v3), and they are identical to noDD except for the applied freshwater forcing. The strengths of the freshwater forcing are 0.2 Sv, 0.1 Sv, and 0.01 Sv respectively in v1, v2, and v3, but the duration and timing of forcing also differs between the simulations. A summary of the forcing periods, the forcing amounts, and total time of each simulation is presented in Table 2. Each simulation was then integrated forward for a minimum of one oscillation to understand the effect of forcing. Specific results for each simulation are described in the following section.

Table 2: Summary of forcing and timing details for each simulation

Simulation Name	Forcing Amount (Sv)	Forcing Period(s) (model years)	Total Run Timespan (model years)
DO.nodd.fwf.v1 (v1)	0.2	2550-2700	2475-3800
DO.nodd.fwf.v2 (v2)	0.1	2550-2700 3880-4030	2475-4600
DO.nodd.fwf.v3 (v3)	0.01	2660-3460	2475-3800

For all simulations, freshwater forcing of various strengths was applied to the same region, though at different times. The specific region is illustrated in Figure 13 and is generally in line with the Ruddiman belt illustrated in Figure 5. This region was picked due to the idea that smaller ice calving events during D-O events (Bond and Lotti, 1995) could offer forcing through the form of icebergs being injected into that region. These icebergs would flow through the Hudson Strait and melt in the shaded region in Figure 5, introducing a source of freshwater. Furthermore, the availability of existing NetCDF files specifying the forcing in that region made it the attractive area to force at the time. Due to the time constraints of the project, this was the only region that was explored for forcing. Further motivation for this choice and its validity are presented in the discussion.

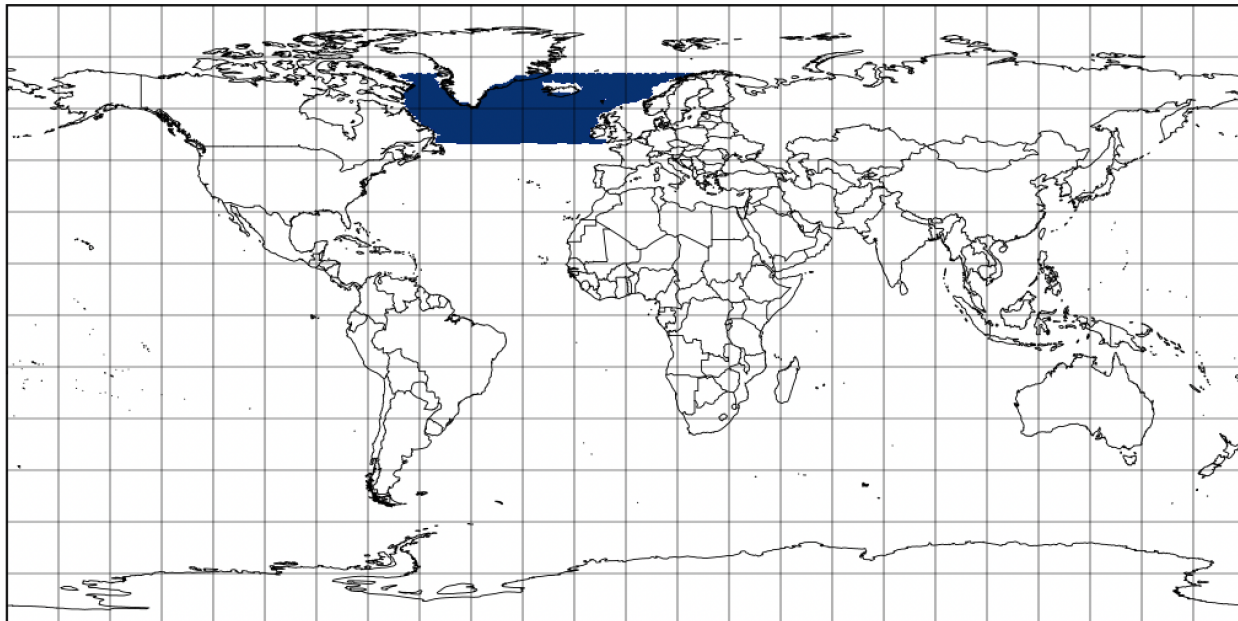


Figure 13: The blue shaded region is the Ruddiman belt of the North Atlantic, where freshwater forcing was applied in simulations v1, v2, v3

5. Results

The following sections detail the findings from each model run. For each model run, the qualitative impact of the freshwater forcing on the shape of the oscillation is discussed. Additionally, modelled regional and global temperature data are produced when relevant to examine the impacts of the forcing. Overall, the aim of this section is to examine if the freshwater forcing shaped the pulses in interesting ways when compared to the earlier simulations of Peltier et al. (2020).

5.1 Freshwater forcing of 0.2 Sv (v1)

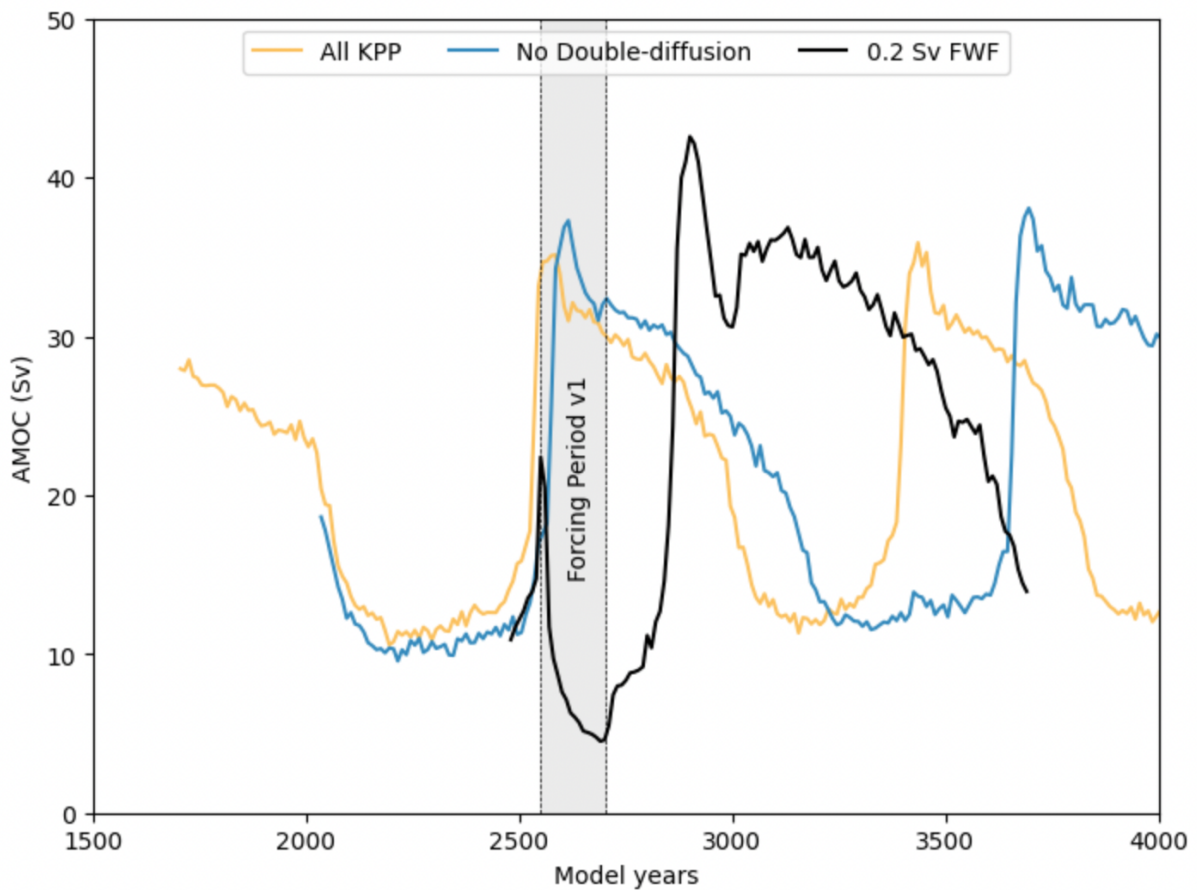


Figure 14: AMOC strength in the simulation where a forcing of 0.2 Sv was applied during the stadial-interstadial transition (shaded region) compared with the AMOC strengths of two “infinite-Q” DO simulations from Peltier et al. (2020)

After running v1 without freshwater forcing for 75 years, freshwater at a rate of 0.2 Sv was introduced for 150 years to the North Atlantic. This forcing is applied “in-phase” with the stadial to interstadial transition. Afterwards, the simulation was continued, with forcing off, up to

model year 3800. Figure 14 compares the simulated AMOC from this experiment to the results from Peltier et al. (2020). As seen in the figure, the forcing of 0.2 Sv was very strong and rapidly attenuated the AMOC strength, drastically impacting the shape of the pulse. This result is quite interesting as it produced an essentially instantaneous near shutoff of the AMOC. Consequently, it was recognized that 0.2 Sv of forcing was too large to more subtly shape the pulse.

Nevertheless, v1 demonstrates the large impact that freshwater forcing has on the AMOC. Figure 15 plots the simulated temperatures at the locations of ice core drilling sites in Greenland (NGRIP) and East Antarctica (EDML). It can be seen that the onset of peak warming in Antarctica for this single oscillation leads the peak warming in Greenland by about one hundred years. This differs from the results in Figure 11, where the peak warmings in both hemispheres are in-phase. Another observation from Figure 15 is that the Greenland temperatures closely mirror the shape of AMOC strength, though the temperature fluctuations are more drastic than those from Figure 11, with the maximum simulated NGRIP temperature easily being over 1°C larger in v1. This simulation was stopped at year 3800 as 0.2 Sv of forcing was evidently too strong to shape the pulses as intended.

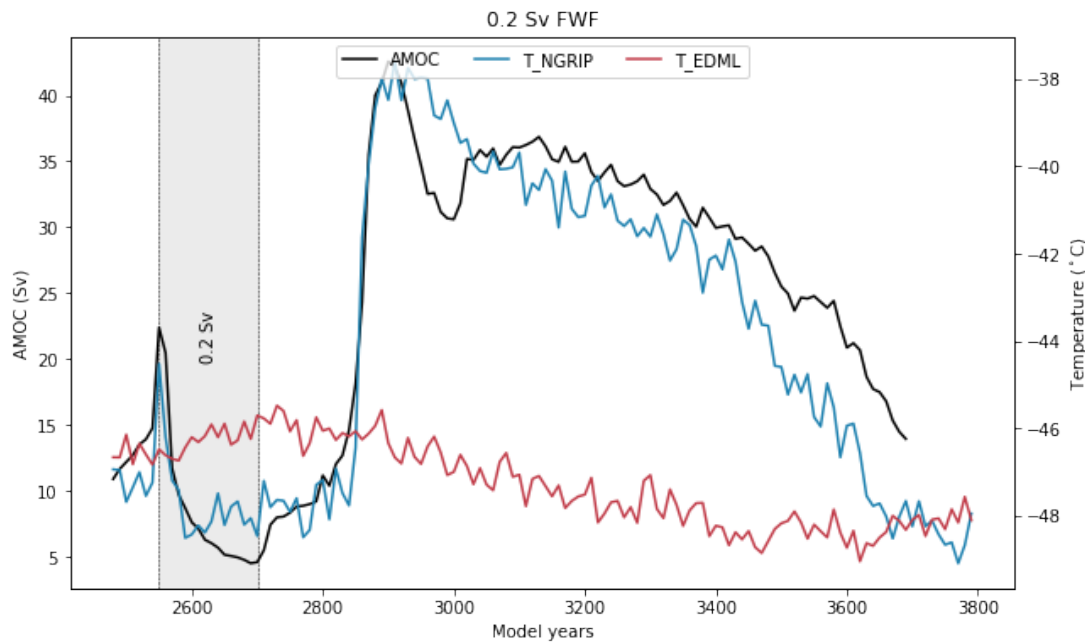


Figure 15: AMOC strength (black) and temperature fluctuations at the NGRIP (blue) and EDML (red) ice core sites in v1.

5.2 Freshwater forcing of 0.1 Sv (v2)

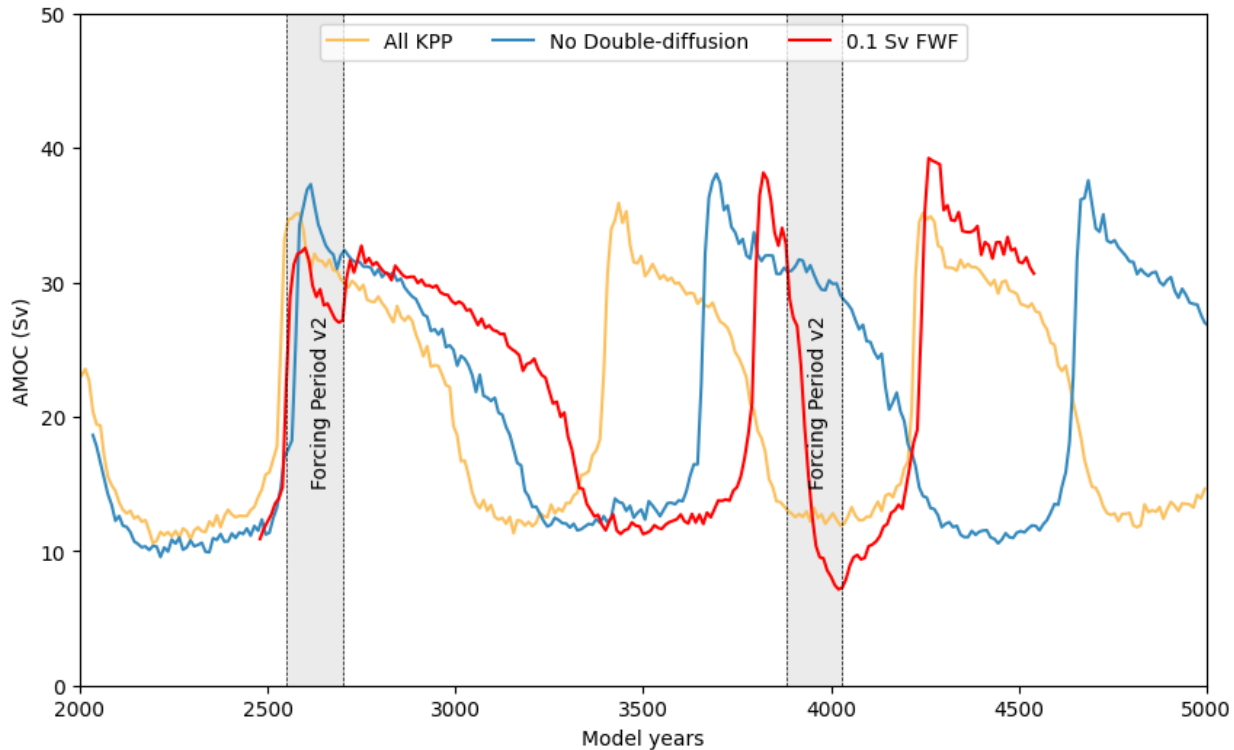


Figure 16 AMOC strength in the simulation where a forcing of 0.1 Sv was applied in phase with the stadial to interstadial transition (first pulse from left) and with a lag (after the completion of the transition; second pulse) compared with the AMOC strengths of two “infinite-Q” DO simulations from Peltier et al. (2020)

As a result of 0.2 Sv being too much forcing, 0.1 Sv of forcing was utilized for the exact same duration and at the same location in the first pulse of v2 model. This simulation (Figure 16) was integrated up to model year 4600, and it can be seen in the first pulse that this forcing did not reduce the AMOC strength as strongly or as quickly as the 0.2 Sv forcing. It did however reduce the amplitude of AMOC strength for the duration of the forcing when compared to the results from Peltier et al. (2020) that had no forcing. The AMOC strength then shoots back up once the forcing stops. With this first pulse, it appears that after the AMOC shoots back up after the termination of the forcing, the slow transition from the interstadial to stadial becomes slower. This is an interesting result, as it could potentially mean that freshwater forcing is responsible for the first oscillation (in the series of oscillations after a Heinrich event) having of a longer period than the subsequent oscillations (if the subsequent ones have reduced amounts of forcing). The period of this first pulse is extended by about 150 years, which is the same length of time as the forcing. Figure 17 shows the simulated temperatures for the simulation in Greenland (NGRIP)

and Antarctica (EDML), along with AMOC strength. Once again, the Greenland temperatures follow the AMOC trend quite closely, and it appears that the Antarctic temperatures reach peaks at approximately the same time as the Greenland ones, so the two hemispheres are in-phase. Comparing this to Figure 11, it can be seen that the initial “overshoot” after the stadial to interstadial transition is not as pronounced, whether it be in terms of temperature or AMOC strength. An additional plot comparing global temperatures during this “overshoot” phase between the noDD simulation from Peltier et al. (2020) and v2 shows how the North Atlantic Region is significantly warmer in the noDD simulation (Figure 18). Furthermore, the temperature trend in this first pulse shows a double peak, and a more gradual decline whereas the ice-core record temperatures have a single sharp peak and a steeper decline. Consequently, the first oscillation in v2 does not meet the temperature constraints in the North Atlantic.

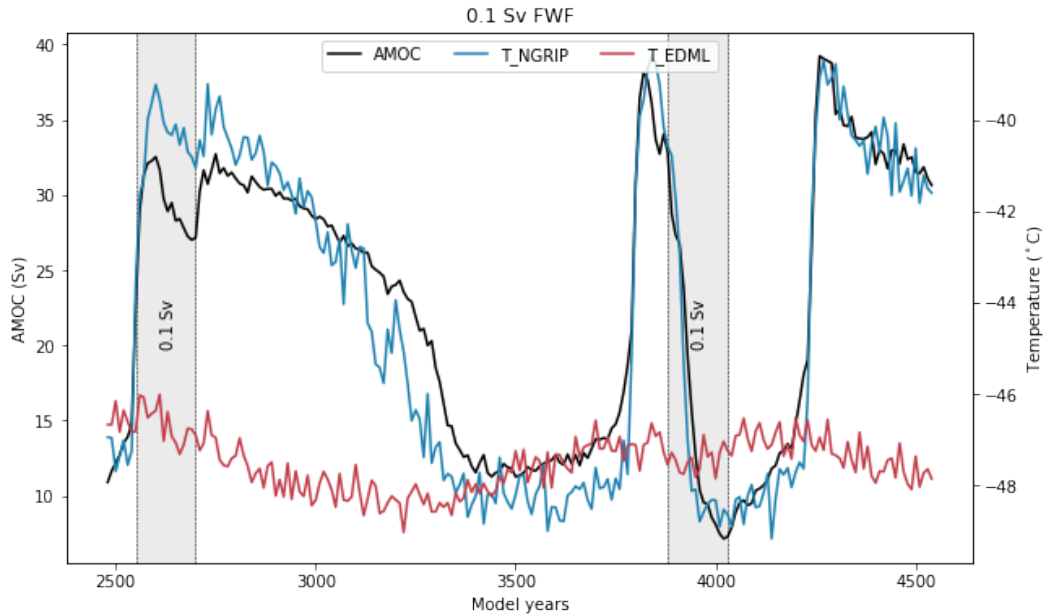


Figure 17: AMOC strength (black) and temperature fluctuations at the NGRIP (blue) and EDML (red) ice core sites in v2

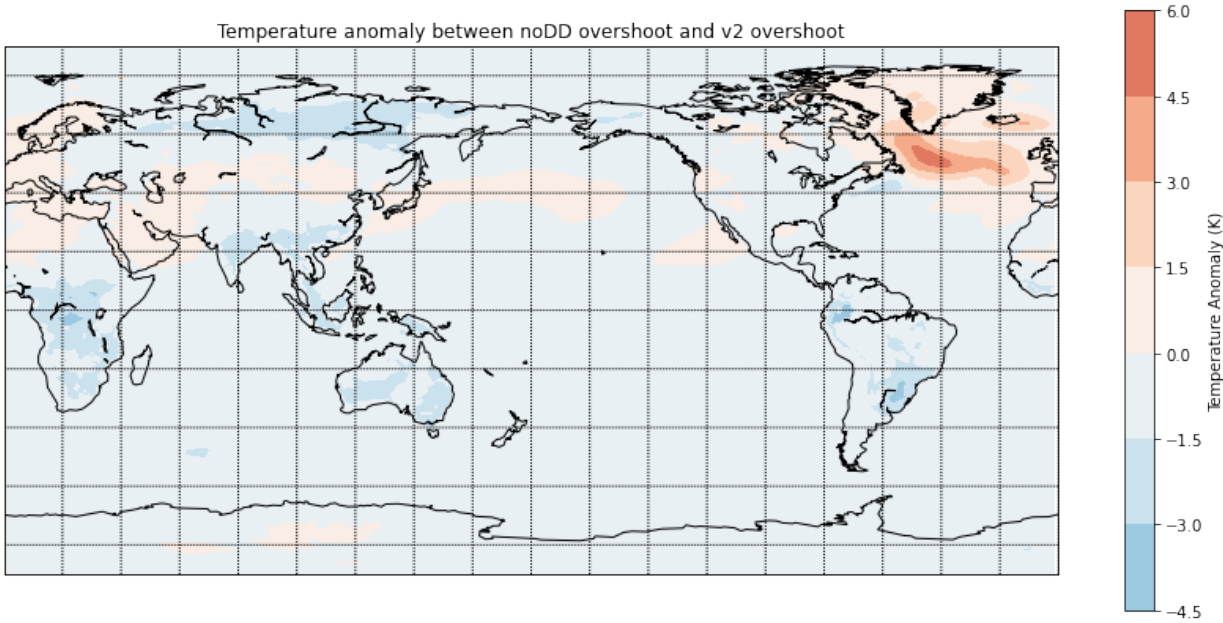


Figure 18: Global temperature anomaly plot obtained by subtracting the v2 overshoot (model years 2560-2610) from the noDD overshoot (model years 2590-2640). This illustrates how the temperatures in the North Atlantic are warmer in the noDD overshoot compared to the v2 overshoot.

Another insight resulting from applying freshwater forcing during the stadial to interstadial transition is that this transition occurs very quickly, so it does not make sense for freshwater forcing to respond immediately (if the source was continental ice sheets reacting to the increase in temperature, for example). Consequently, during the second pulse, a lag of roughly 100 years was added before introducing the same 0.1 Sv of forcing. This second forcing period can be seen in Figures 16 and 17. A shifted version of this second pulse can be seen in Figure 19 to better illustrate the impact of this lagged forcing on the period of the pulse compared with the results from Peltier et al. (2020).

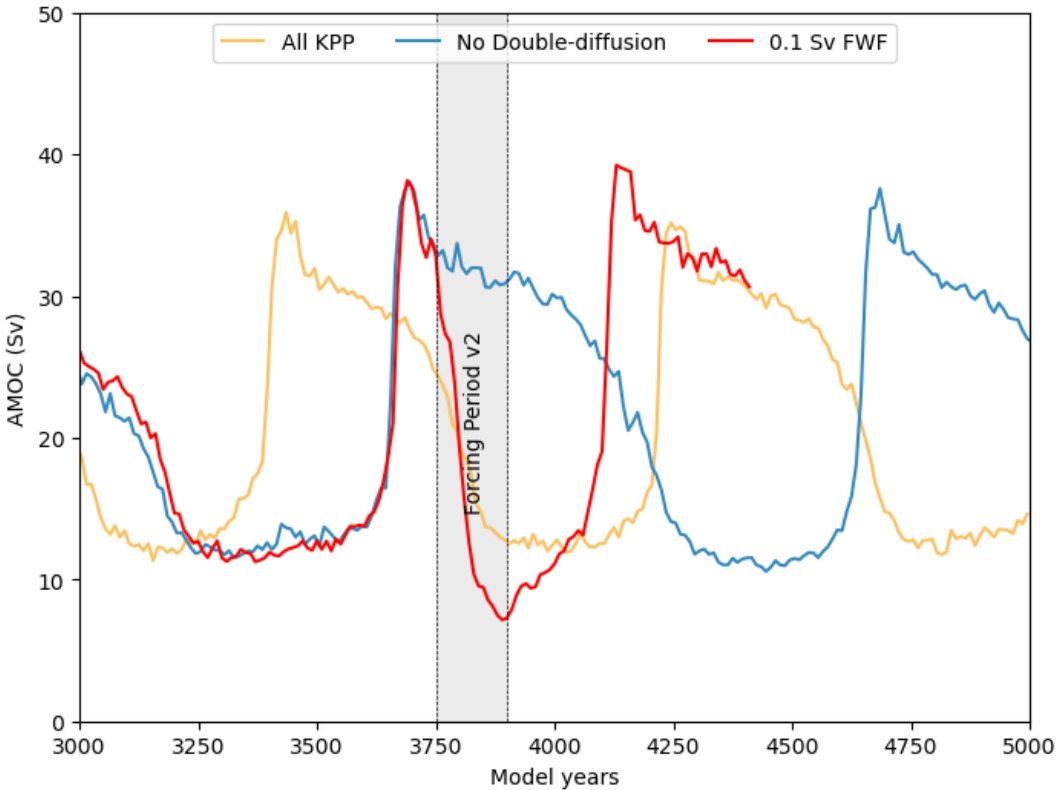


Figure 19: Shifting the v2 time series forward by 130 years to align the second v2 pulse with the second noDD pulse. This is to better illustrate the change in period as a result of the lagged forcing

What can be seen from Figure 19 is that this lagged forcing quickly depressed the AMOC, and actually lowered the stadial AMOC strength compared to the preceding stadial, though temperatures at the NGRIP site were not significantly impacted (seen in Figure 17). Expanding this to global temperatures, the reduced stadial in v2 did result in slightly lower temperatures in the Northern Hemisphere than the first v2 stadial, which is shown to be warmer in Figure 20. The occurrence of a stadial that is colder than earlier stadials is quite similar to the behaviour of some of the oscillations in $\delta^{18}\text{O}$ illustrated in Figure 1. Notable examples in Figure 1 are pulses 8, 9, and 10 in MIS 3, whose stadials after the pulse are colder than the stadials prior to the pulse. Unlike the forcing during the stadial to interstadial transition which only extended the period by 150 years (the same amount of time as the forcing), this lagged forcing shortened the period of the pulse by a significant amount. The timing between the peaks of the second and third pulse in v2 is about 500 years shorter than the timing between the peaks of the second and third pulse in noDD. Comparing the in-phase forcing results with the lagged forcing results, it

can be seen that the in-phase forcing slows the upward “momentum” of the AMOC, which dampens the overshoot seen in the previous results. For the lagged forcing, it is in trend with downward “momentum” of the AMOC, so it rapidly depresses the AMOC and forms an “undershoot”. Consequently, the results from v2 demonstrate how freshwater forcing can shape the pulses based on the time at which forcing is introduced.

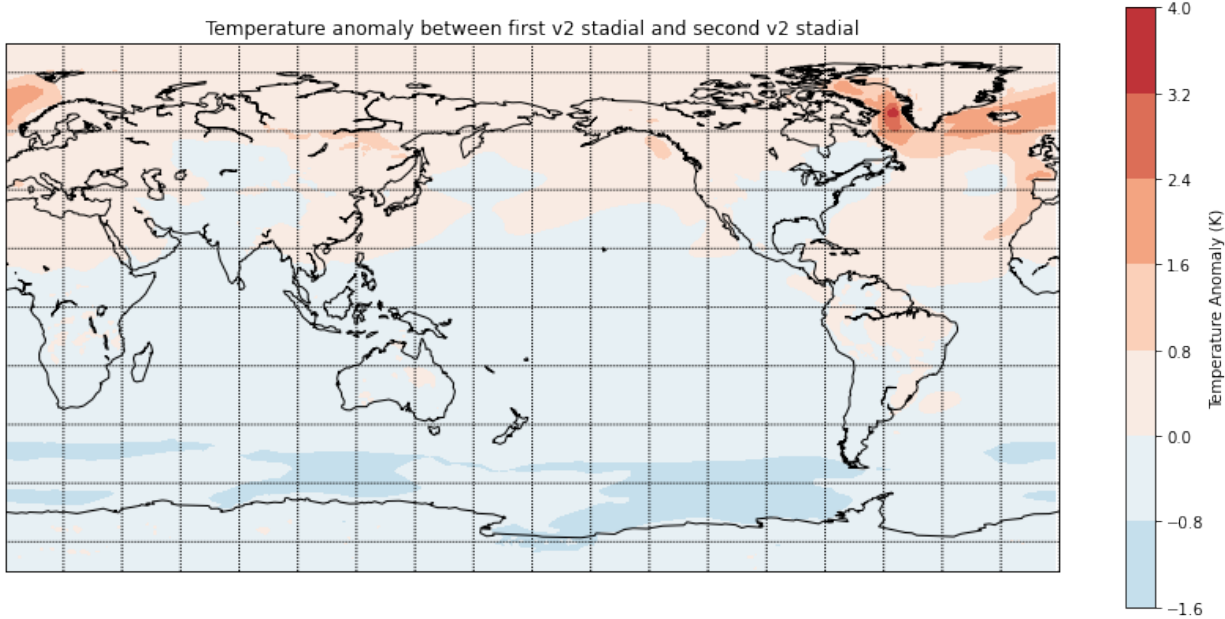


Figure 20: Global temperature anomaly plot obtained by subtracting the second v2 stadial (model years 3980-4080) from the first v2 stadial (model years 3500-3600). This illustrates how the temperatures in the North Atlantic are colder in the second stadial compared to the first.

5.3 Freshwater forcing of 0.01 Sv (v3)

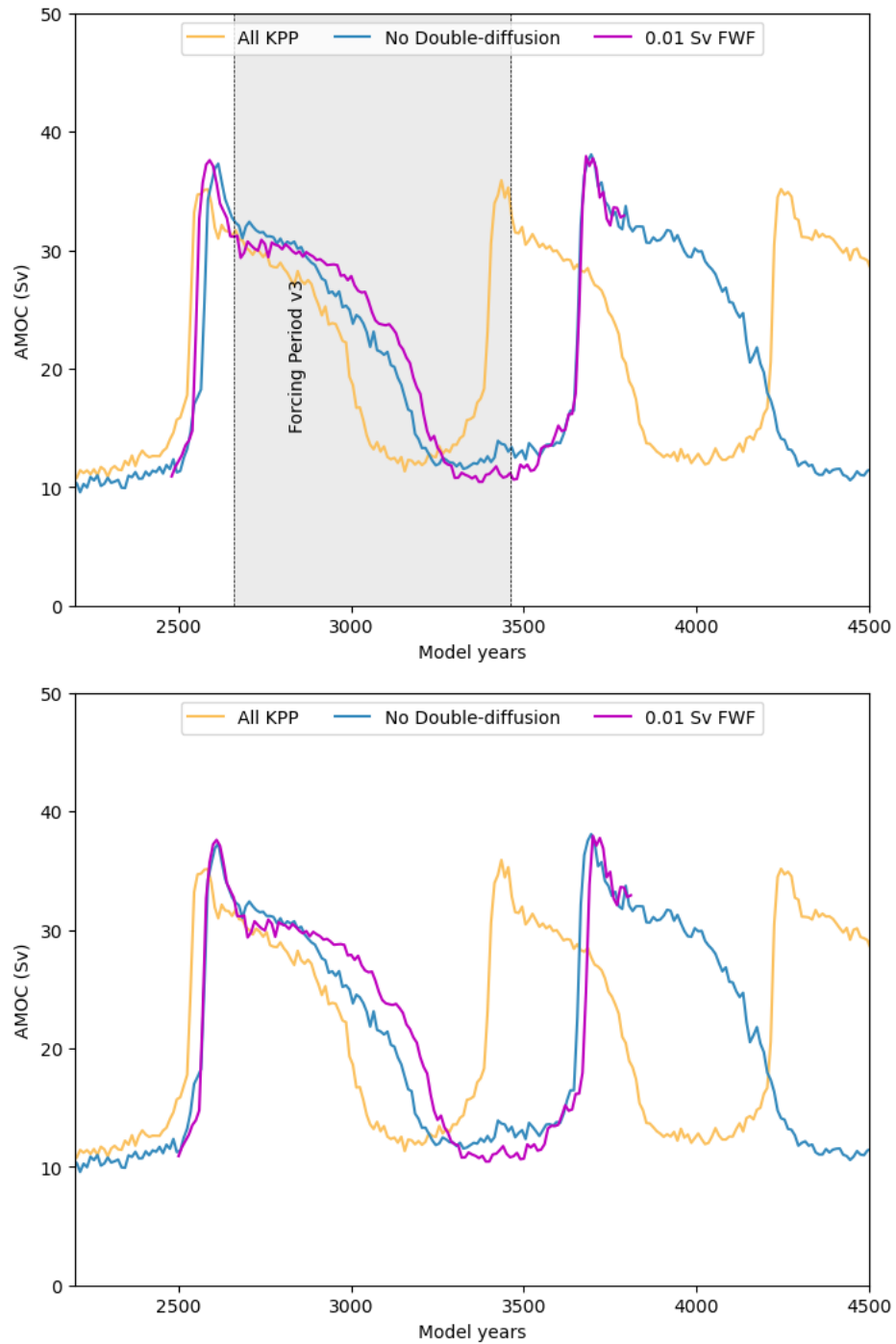


Figure 21: AMOC strength in the simulation with a forcing of 0.01 Sv (top) and the same time series shifted back by 20 years (bottom) compared with the AMOC strengths of two “infinite-Q” DO simulations from Peltier et al. (2020)

Recognizing that 0.1 Sv and 0.2 Sv of forcing (whether applied in phase with the stadial to interstadial transition or applied with a lag) significantly altered pulse shape, a lagged forcing of 0.01 Sv was introduced in the third and final simulation to investigate the effects of a much smaller forcing amount. This forcing continued for 800 model years, until the first pulse terminated. This was because the AMOC had re-entered stadial conditions, so the forcing was expected to stop. The entire simulation ran up until model year 3800 in which the peak of the second pulse can be seen and used to determine how the forcing affected the period of the pulses. The AMOC response compared with the results of Peltier et al. (2020), can be seen in Figure 21. Quite interestingly, the additional freshwater forcing resulted in no attenuation of AMOC strength, especially when compared with the lagged 0.1 Sv forcing from v2. In fact, as seen in Figure 21, when the first peak of v3 is aligned with the first peak of the noDD run from Peltier et al. (2020), the period between the two peaks in v3 is extended to be 20 years longer than the noDD period. This is the same amount that the v3 series was shifted by to align it with the first noDD pulse. If this alignment does not occur, it can be seen that the second pulse is directly aligned with the second noDD pulse, further indicating that this forcing had minimal effect. Another observation to note is that the second stadial appears to have a weaker AMOC than the first, in a similar manner to that of the second pulse from v2. However, this does not translate to drastic temperature changes. Comparing the stadial after the first pulse in the v3 simulation with the stadial after the first pulse in the noDD simulation, the noDD stadial is only marginally warmer in the North Atlantic (Figure 22). Finally, the temperatures at NGRIP and EDML during this run are found in Figure 23. Since this forcing had minimal impact on the AMOC, these temperatures are resultingly quite similar to those of the noDD simulation. The NGRIP temperature follows the AMOC strength, and the EDML temperature peaks occur in-phase with peak NGRIP temperatures. It can therefore be seen that the lagged forcing of 0.01 Sv had a relatively minimal effect on the simulated pulse shapes and temperatures.

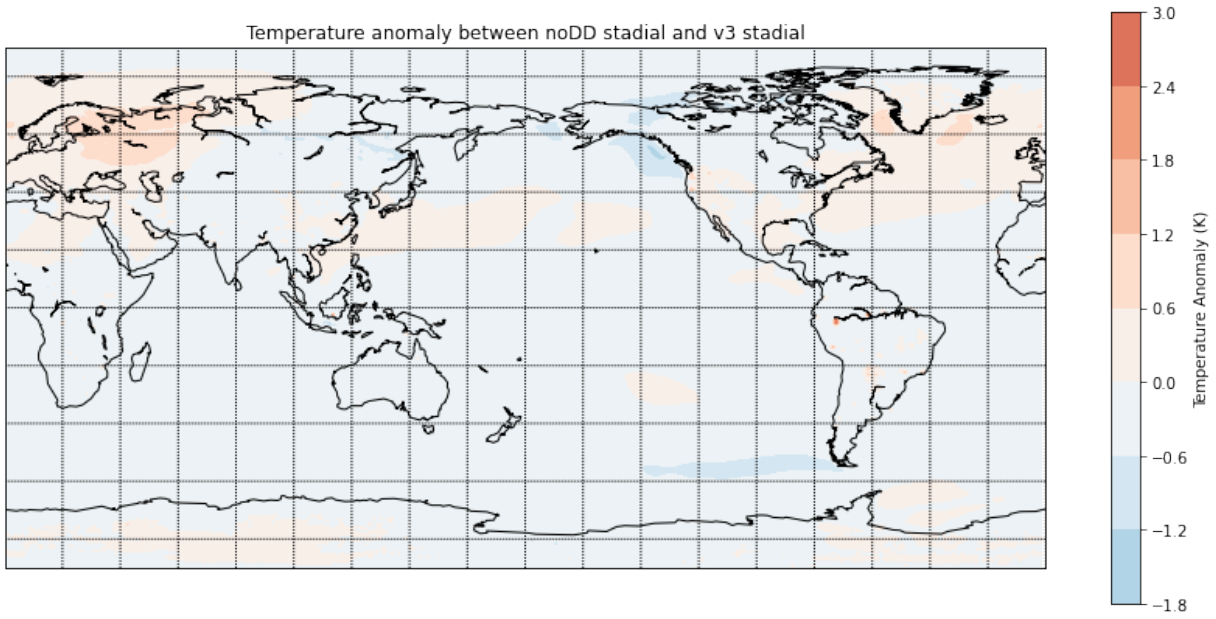


Figure 22: Global temperature anomaly plot obtained by subtracting the v3 stadial (model years 3350-3450) from the noDD stadial (model years 3300-3400). It shows how the v3 stadial is only marginally colder than the noDD stadial in the North Atlantic

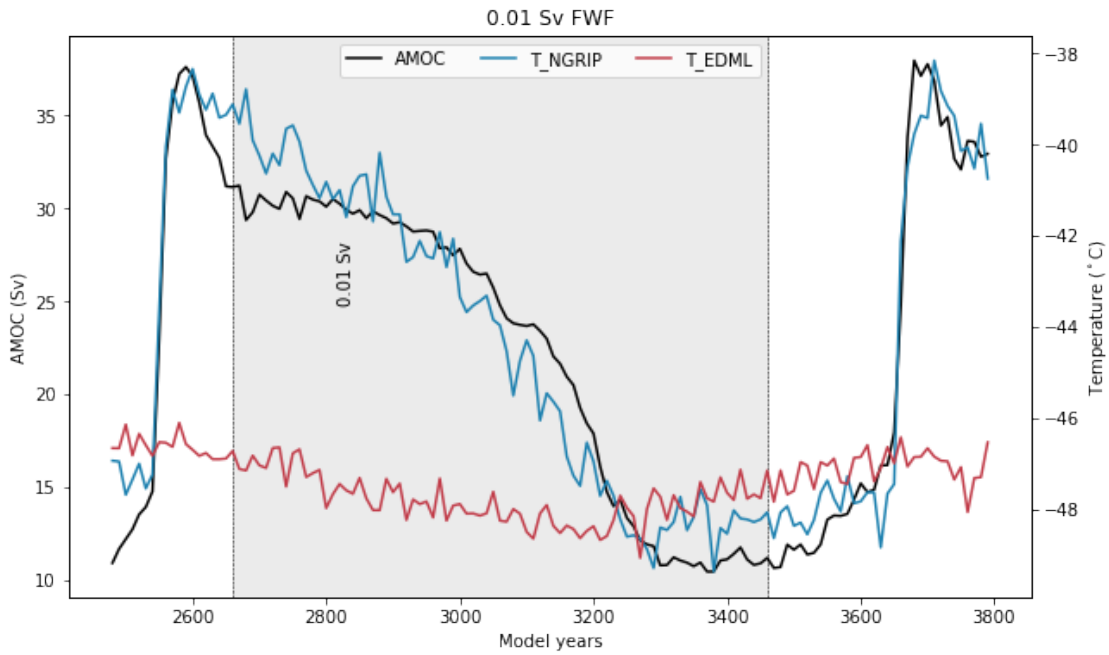


Figure 23: AMOC strength (black) and temperature fluctuations at the NGRIP (blue) and EDML (red) ice core sites in v3

6. Discussion

Evidently, given the time constraints of this project, many other pathways to shaping the periods and amplitudes of these pulses have not been explored. This discussion will first examine the implications of the simulation results, before discussing further paths to investigate. The most obvious takeaway from these experiments is that a range of effects on the pulse shape due to freshwater forcing has been identified. Strong freshwater forcing, like 0.2 Sv in the v1 simulation, can weaken the AMOC even when applied in-phase with the stadial to interstadial transition. On the other hand, 0.1 Sv of forcing during the transition did not result in a weakened AMOC, though the upwards “momentum” of the AMOC was reduced and the “overshoot” was smaller than those of unforced pulses. A similar behaviour can be seen with lagged forcing as 0.1 Sv of freshwater, when applied with a lag, rapidly weakened the AMOC whereas 0.01 Sv of forcing had no weakening at all compared to the simulations with no forcing. Therefore, this project determined two ranges of forcing that can significantly shape the pulses; one range for forcing applied during the stadial to interstadial transition, and another for a lagged forcing. Within these ranges, there lies possible thresholds for forcing to significantly alter the strength of the AMOC. For freshwater forcing to the North Atlantic during the stadial to interstadial transition, a threshold somewhere between 0.1 Sv and 0.2 Sv will cause a rapid weakening of the AMOC. For the lagged forcing, this threshold lies somewhere between 0.01 Sv and 0.1 Sv. Therefore, further opportunities exist to test additional amounts of forcing to identify these thresholds. Once that better understanding is obtained, one can use freshwater forcing to shape the pulse, whether it be applied during the fast stadial to interstadial transition or during the more gradual interstadial to stadial transition. These modifications could then shape the perfectly periodic oscillations observed in Peltier et al. (2020) to be closer to the oscillations observed in ice core records.

These experiments relied on the assumption that freshwater forcing is introduced in the form of icebergs discharged from the Hudson strait. Though millennial scale iceberg discharges do occur (Bond and Lotti, 1995), it is unclear if they coincide with stadials or interstadials (McCabe and Clark, 1998; Clarke et al. 1999). Modelling has shown the peak 100-year discharge during the last glacial cycle to be 0.12 Sv (Marshall and Koutnik, 2006), which is of the same order of magnitude as the v2 simulation that forced 0.1 Sv. Furthermore, their mean discharge to

the North Atlantic was 0.06 Sv between 60-20 kyr BP (Marshall and Koutnik, 2006), so the forcing of 0.01 Sv used in v3 could probably correspond with periods of minimal discharge. Most importantly, Marshall and Koutnik (2006) note that iceberg fluxes were at a maximum during the stadials, and that there was little iceberg flux during interstadials. This means that it is not likely for 0.1 Sv of forcing (in v2) to be applied during the interstadial through icebergs. However, the 0.01 Sv of forcing in v3 could still be viable, though as shown earlier, it has minimal impact to the AMOC. As a result, forcing applied directly to the North Atlantic is unlikely the main mechanism that shapes the pulses.

An aspect of freshwater forcing that was overlooked in this project's scope is the introduction of meltwater in areas outside of the North Atlantic. Meltwater coming from continental ice sheets could shape the pulses in a similar manner as the freshwater introduced directly to the North Atlantic. A significant source of meltwater during MIS 3 is the Laurentide Ice Sheet (LIS). The LIS has five main routes for meltwater: the Mississippi River, the Hudson River, the St. Lawrence River, the Mackenzie River, and the Hudson Strait (Licciardi et al., 1999). Clark et al (2001) hypothesized that a switching of routes between the Mississippi River (which flows into the Gulf of Mexico) and the Hudson or St. Lawrence Rivers (which flows into the North Atlantic) was the mechanism behind climate variability in the last glaciation. Regardless of where or if this switching occurs, the Mississippi would be the main outlet during interstadials. Flower et al. (2011) show that the Mississippi is the main outlet of LIS meltwater throughout MIS 3, and that it is unlikely the main mechanism driving D-O oscillations. This agrees with the results from Peltier and Vettoretti (2014) in that there is no need for freshwater forcing to create D-O-like oscillations. However, this meltwater into the Gulf of Mexico during the interstadials could perhaps be the extra factor that shapes the oscillations in ways similar to that of the simulations from this project. This could potentially yield oscillations with a “finite-Q” similar to that of the ice core profiles, rather than an “infinite-Q” in the existing Peltier et al. (2020) model. Consequently, further simulations should try adding additional freshwater forcing to the Gulf of Mexico to see if it can similarly shape the pulses. Outside of the Laurentide Ice Sheet, ice sheets surrounding the Nordic Seas also have been shown to have increased meltwater discharge during interstadials (Rasmussen and Thomsen, 2013). This then offers yet another possible location for the application of freshwater forcing in future simulations.

As mentioned in the interim report, further investigations could also examine how a time varying freshwater forcing impacts the pulse shape. This is based off the idea that the freshwater forcing response is tied with the temperature, so as the temperature gradually drops back to stadial conditions from the interstadial, the amount of meltwater would reduce. This proposed time varying forcing is illustrated in Figure 24. However, in order to correctly apply this time varying forcing, a more concrete understanding of how much forcing and where to apply it is needed. Although this project has identified a range of forcing that can alter the pulse shape, this range needs to be examined further to identify potential thresholds where significant impact to the AMOC could occur, as discussed earlier. This, along with better understanding of the area to force, would then allow for additional modifications to the forcing such as adding a time varying element.

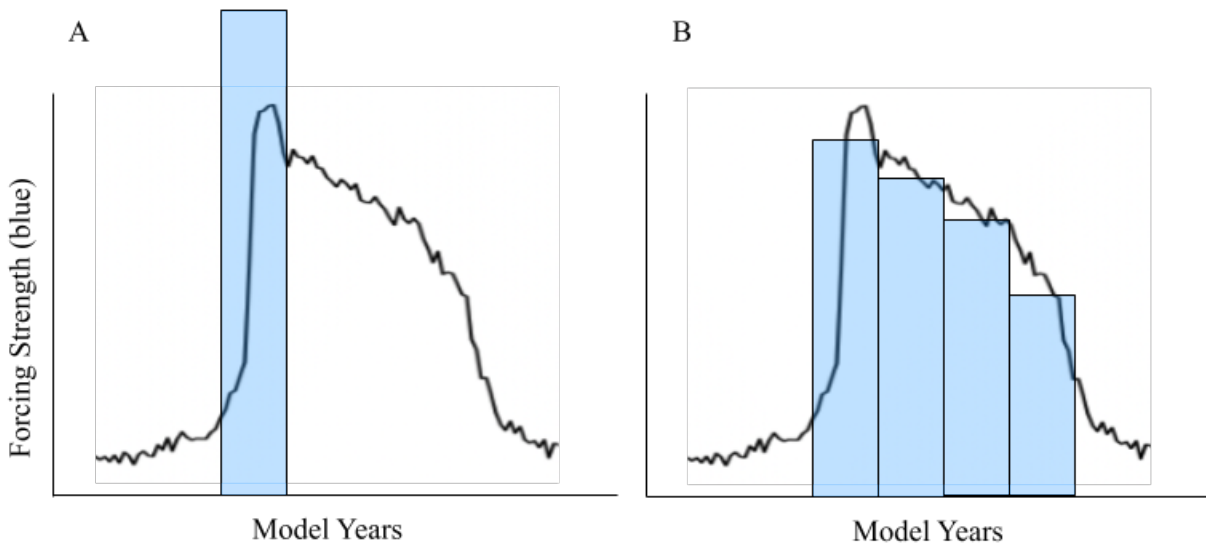


Figure 24: Rather than having one large freshwater forcing pulse (marked in blue) (A) for 150 years, one could potentially introduce smaller amounts of forcing that change in accordance with AMOC strength (black line) (B) (drawings not to scale)

7. Conclusions

The goal at the onset of this project was to see if a physically plausible freshwater injection scenario can be developed to shape the results from Peltier et al. (2020) to more closely mimic the D-O oscillations identified in the Greenland ice cores. More specifically, this project focused on seeing if freshwater forcing could control the period and amplitude of individual pulses, thus shaping them to have the “finite-Q” that is observed in the cores. The main finding from this project is the identification of ranges of freshwater forcing amounts that can reasonably change the shapes of the pulses when applied directly to the North Atlantic. This project qualitatively identified how various amounts of freshwater could change the pulse shape based off the amount of forcing, and when the forcing is introduced. Although direct freshwater forcing to the North Atlantic is unlikely the main mechanism behind the “finite-Q” of these oscillations, the simulations from this project offer proof that freshwater can significantly change pulse shape and could potentially shape them into the desired forms. Therefore, the ranges of forcing determined from this project offers potential constraints for future simulations. In terms of future simulations, a priority would be examining the effects of forcing in different areas in addition to trying different forcing patterns. Then, through the usage of different forcing amounts, timings, areas, and patterns, a more comprehensive understanding of how freshwater forcing shapes D-O pulses can be achieved. This project offers a stepping stone in the form of investigating different forcing amounts and timings.

The investigation of D-O oscillations in climate simulations is important in understanding the climate of today. This project has demonstrated how the AMOC is quite sensitive to freshwater forcing, and regional temperatures are heavily correlated with AMOC strength. Therefore, in identifying all the factors that shape the D-O oscillations, a better understanding of its mechanisms will be reached. This includes further understanding of the AMOC, which is relevant for understanding today’s climate. In fact, a recent communication by Caesar et al. (2021) asserts that the AMOC is currently at its weakest in the past millennium, and that this slowdown is quite unprecedented. Consequently, studies like this project that strive to understand the AMOC through paleoclimate phenomena like D-O oscillations could help improve the understanding of the current slowdown. Overall, further investigations through the modelling of paleoclimate are key in growing our understanding of the current climate.

8. References

- Alley, R. B., Anandakrishnan, S., & Jung, P. (2001). Stochastic resonance in the North Atlantic. *Paleoceanography*, 16(2), 190-198. doi:10.1029/2000pa000518
- Alley, R. B., & Clark, P. U. (1999). The deglaciation of the northern hemisphere: A global perspective. *Annual Review of Earth and Planetary Sciences*, 27(1), 149-182. doi:10.1146/annurev.earth.27.1.149
- Argus, D. F., Peltier, W. R., Drummond, R., & Moore, A. W. (2014). The Antarctica component of postglacial rebound model ICE-6g_c (VM5a) based on GPS positioning, exposure age dating of ice thicknesses, and relative sea level histories. *Geophysical Journal International*, 198(1), 537-563. doi:10.1093/gji/ggu140
- Barker, S., Chen, J., Gong, X., Jonkers, L., Knorr, G., & Thornalley, D. (2015). Icebergs not the trigger for North Atlantic cold events. *Nature*, 520(7547), 333-336. doi:10.1038/nature14330
- Bjerknes, V. (1910). *Dynamic meteorology and hydrography*.
- Blunier, T., Chappellaz, J., Schwander, J., Dällenbach, A., Stauffer, B., Stocker, T. F., ... Johnsen, S. J. (1998). Asynchrony of Antarctic and Greenland climate change during the last glacial period. *Nature*, 394(6695), 739-743. doi:10.1038/29447
- Bond, G. C., & Lotti, R. (1995). Iceberg discharges into the North Atlantic on millennial time scales during the last glaciation. *Science*, 267(5200), 1005-1010. doi:10.1126/science.267.5200.1005
- Broecker, W. S. (1998). Paleocean circulation during the last Deglaciation: A bipolar seesaw? *Paleoceanography*, 13(2), 119-121. doi:10.1029/97pa03707
- Broecker, W. S., Bond, G., Klas, M., Bonani, G., & Wolfli, W. (1990). A salt oscillator in the glacial Atlantic? 1. The concept. *Paleoceanography*, 5(4), 469-477. doi:10.1029/pa005i004p00469
- Broecker, W. S., & Denton, G. H. (1989). The role of ocean-atmosphere reorganizations in glacial cycles. *Geochimica et Cosmochimica Acta*, 53(10), 2465-2501. doi:10.1016/0016-7037(89)90123-3
- Broecker, W. S., Peteet, D. M., & Rind, D. (1985). Does the ocean-atmosphere system have more than one stable mode of operation? *Nature*, 315(6014), 21-26. doi:10.1038/315021a0
- Brown, N., & Galbraith, E. D. (2016). Hosed vs. unhosed: Interruptions of the Atlantic meridional overturning circulation in a global coupled model, with and without freshwater forcing. *Climate of the Past*, 12(8), 1663-1679. doi:10.5194/cp-12-1663-2016

- Buckley, M. W., & Marshall, J. (2016). Observations, inferences, and mechanisms of the Atlantic meridional overturning circulation: A review. *Reviews of Geophysics*, 54(1), 5-63. doi:10.1002/2015rg000493
- Budyko, M. I. (1969). The effect of solar radiation variations on the climate of the earth. *Tellus*, 21(5), 611-619. doi:10.3402/tellusa.v21i5.10109
- Caesar, L., McCarthy, G. D., Thornalley, D. J., Cahill, N., & Rahmstorf, S. (2021). Current Atlantic meridional overturning circulation weakest in last millennium. *Nature Geoscience*, 14(3), 118-120. doi:10.1038/s41561-021-00699-z
- Clark, P. U., Marshall, S. J., Clarke, G. K., Hostetler, S. W., Licciardi, J. M., & Teller, J. T. (2001). Freshwater forcing of abrupt climate change during the last glaciation. *Science*, 293(5528), 283-287. doi:10.1126/science.1062517
- Clarke, G. K., Marshall, S. J., Hillaire-Marcel, C., Bilodeau, G., & Veiga-Pires, C. (1999). A glaciological perspective on Heinrich events. *Mechanisms of Global Climate Change at Millennial Time Scales*, 243-262. doi:10.1029/gm112p0243
- Dansgaard, W. (1954). The O₁₈-abundance in fresh water. *Geochimica et Cosmochimica Acta*, 6(5-6), 241-260. doi:10.1016/0016-7037(54)90003-4
- Dansgaard, W., Clausen, H. B., Gundestrup, N., Hammer, C. U., Johnsen, S. F., Kristinsdottir, P. M., & Reeh, N. (1982). A new Greenland deep ice core. *Science*, 218(4579), 1273-1277. doi:10.1126/science.218.4579.1273
- Dansgaard, W., Johnsen, S. J., Moller, J., & Langway, C. C. (1969). One thousand centuries of climatic record from camp century on the Greenland ice sheet. *Science*, 166(3903), 377-380. doi:10.1126/science.166.3903.377
- Dansgaard, W., Johnsen, S. J., Clausen, H. B., Dahl-Jensen, D., Gundestrup, N. S., Hammer, C. U., ... Bond, G. (1993). Evidence for general instability of past climate from a 250-kyr ice-core record. *Nature*, 364(6434), 218-220. doi:10.1038/364218a0
- Dansgaard, W., White, J. W., & Johnsen, S. J. (1989). The abrupt termination of the younger Dryas climate event. *Nature*, 339(6225), 532-534. doi:10.1038/339532a0
- Delworth, T. L., Clark, P. U., Holland, M., Johns, W. E., Kuhlbrodt, T., Lynch-Stieglitz, J., ... Zhang, R. (2008). The Potential for Abrupt Change in the Atlantic Meridional Overturning Circulation. In *Abrupt Climate Change* (pp. 258-359). Retrieved from https://www.gfdl.noaa.gov/bibliography/related_files/td0802.pdf
- Drijfhout, S., Gleeson, E., Dijkstra, H. A., & Livina, V. (2013). Spontaneous abrupt climate change due to an atmospheric blocking-sea-ice-ocean feedback in an unforced climate

model simulation. *Proceedings of the National Academy of Sciences*, 110(49), 19713-19718. doi:10.1073/pnas.1304912110

Edwards, P. N. (2010). History of climate modeling. *Wiley Interdisciplinary Reviews: Climate Change*, 2(1), 128-139. doi:10.1002/wcc.95

EPICA Community Members. (2006). One-to-one coupling of glacial climate variability in Greenland and Antarctica. *Nature*, 444(7116), 195-198. doi:10.1038/nature05301

Fletcher, W. J., Sánchez Goñi, M. F., Allen, J. R., Cheddadi, R., Combourieu-Nebout, N., Huntley, B., ... Tzedakis, P. (2010). Millennial-scale variability during the last glacial in vegetation records from Europe. *Quaternary Science Reviews*, 29(21-22), 2839-2864. doi:10.1016/j.quascirev.2009.11.015

Flower, B. P., Williams, C., Hill, H. W., & Hastings, D. W. (2011). Laurentide ice sheet Meltwater and the Atlantic meridional overturning circulation during the last glacial cycle: A view from the Gulf of Mexico. *Abrupt Climate Change: Mechanisms, Patterns, and Impacts*, 39-56. doi:10.1029/2010gm001016

Galbraith, E. D., Kwon, E. Y., Gnanadesikan, A., Rodgers, K. B., Griffies, S. M., Bianchi, D., ... Held, I. M. (2011). Climate variability and radiocarbon in the CM2Mc earth system model. *Journal of Climate*, 24(16), 4230-4254. doi:10.1175/2011jcli3919.1

Ganopolski, A., & Rahmstorf, S. (2001). Rapid changes of glacial climate simulated in a coupled climate model. *Nature*, 409(6817), 153-158. doi:10.1038/35051500

Gent, P. R., Danabasoglu, G., Donner, L. J., Holland, M. M., Hunke, E. C., Jayne, S. R., ... Zhang, M. (n.d.). The Community Climate System Model Version 4. *Journal of Climate*, 24(19), 4973–4991. doi:10.1175/2011JCLI4083.1

Heinrich, H. (1988). Origin and consequences of cyclic ice rafting in the Northeast Atlantic Ocean during the past 130,000 years. *Quaternary Research*, 29(2), 142-152. doi:10.1016/0033-5894(88)90057-9

Hemming, S. R. (2004). Heinrich events: Massive late Pleistocene detritus layers of the North Atlantic and their global climate imprint. *Reviews of Geophysics*, 42(1). doi:10.1029/2003rg000128

Henry, L. G., McManus, J. F., Curry, W. B., Roberts, N. L., Piotrowski, A. M., & Keigwin, L. D. (2016). North Atlantic Ocean circulation and abrupt climate change during the last glaciation. *Science*, 353(6298), 470-474. doi:10.1126/science.aaf5529

Intergovernmental Panel on Climate Change. (2014). *Climate change 2013: The physical science basis: Working group I contribution to the fifth assessment report of the intergovernmental panel on climate change*. Cambridge University Press.

- Johnsen, S. J., Clausen, H. B., Dansgaard, W., Fuhrer, K., Gundestrup, N., Hammer, C. U., ... Steffensen, J. P. (1992). Irregular glacial interstadials recorded in a new Greenland ice core. *Nature*, 359(6393), 311-313. doi:10.1038/359311a0
- Johnsen, S. J., Dahl-Jensen, D., Dansgaard, W., & Gundestrup, N. (1995). Greenland palaeotemperatures derived from GRIP bore hole temperature and ice core isotope profiles. *Tellus B: Chemical and Physical Meteorology*, 47(5), 624-629. doi:10.3402/tellusb.v47i5.16077
- Kageyama, M., Paul, A., Roche, D. M., & Van Meerbeeck, C. J. (2010). Modelling glacial climatic millennial-scale variability related to changes in the Atlantic meridional overturning circulation: A review. *Quaternary Science Reviews*, 29(21-22), 2931-2956. doi:10.1016/j.quascirev.2010.05.029
- Kindler, P., Guillevic, M., Baumgartner, M., Schwander, J., Landais, A., & Leuenberger, M. (2014). Temperature reconstruction from 10 to 120 kyr b2k from the NGRIP ice core. *Climate of the Past*, 10(2), 887-902. doi:10.5194/cp-10-887-2014
- Klockmann, M., Mikolajewicz, U., & Marotzke, J. (2018). Two AMOC states in response to decreasing greenhouse gas concentrations in the coupled climate model MPI-ESM. *Journal of Climate*, 31(19), 7969-7984. doi:10.1175/jcli-d-17-0859.1
- Knutti, R., Flückiger, J., Stocker, T. F., & Timmermann, A. (2004). Strong hemispheric coupling of glacial climate through freshwater discharge and ocean circulation. *Nature*, 430(7002), 851-856. doi:10.1038/nature02786
- Kuhlbrodt, T., Griesel, A., Montoya, M., Levermann, A., Hofmann, M., & Rahmstorf, S. (2007). On the driving processes of the Atlantic meridional overturning circulation. *Reviews of Geophysics*, 45(2). doi:10.1029/2004rg000166
- Le Treut, H., Somerville, R., Cubasch, U., Ding, Y., Mauritzen, C., Mokssit, A., ... Prather, M. (2007). Historical Overview of Climate Change Science. In *Climate Change 2007: The Physical Science Basis. Contribution of Working Group I to the Fourth Assessment Report of the Intergovernmental Panel on Climate Change*. Retrieved from <https://www.ipcc.ch/site/assets/uploads/2018/03/ar4-wg1-chapter1.pdf>
- Lehman, S. J., & Keigwin, L. D. (1992). Sudden changes in North Atlantic circulation during the last deglaciation. *Nature*, 356(6372), 757-762. doi:10.1038/356757a0
- Li, C., & Born, A. (2019). Coupled atmosphere-ice-ocean dynamics in dansgaard-oeschger events. *Quaternary Science Reviews*, 203, 1-20. doi:10.1016/j.quascirev.2018.10.031
- Licciardi, J. M., Teller, J. T., & Clark, P. U. (1999). Freshwater routing by the Laurentide ice sheet during the last deglaciation. *Mechanisms of Global Climate Change at Millennial Time Scales*, 177-201. doi:10.1029/gm112p0177

- Manabe, S., & Bryan, K. (1969). Climate calculations with a combined ocean-atmosphere model. *Journal of the Atmospheric Sciences*, 26(4), 786-789. doi:10.1175/1520-0469(1969)026<0786:ccwaco>2.0.co;2
- Marshall, S. J., & Koutnik, M. R. (2006). Ice sheet action versus reaction: Distinguishing between Heinrich events and Dansgaard-Oeschger cycles in the North Atlantic. *Paleoceanography*, 21(2), n/a-n/a. doi:10.1029/2005pa001247
- McCabe, A. M., & Clark, P. U. (1998). Ice-sheet variability around the North Atlantic Ocean during the last deglaciation. *Nature*, 392(6674), 373-377. doi:10.1038/32866
- McManus, J. F., Francois, R., Gherardi, J., Keigwin, L. D., & Brown-Leger, S. (2004). Collapse and rapid resumption of Atlantic meridional circulation linked to deglacial climate changes. *Nature*, 428(6985), 834-837. doi:10.1038/nature02494
- Meese, D. A., Gow, A. J., Alley, R. B., Zielinski, G. A., Grootes, P. M., Ram, M., ... Bolzan, J. F. (1997). The Greenland ice sheet project 2 depth-age scale: Methods and results. *Journal of Geophysical Research: Oceans*, 102(C12), 26411-26423. doi:10.1029/97jc00269
- Menviel, L. C., Skinner, L. C., Tarasov, L., & Tzedakis, P. C. (2020). An ice-climate oscillatory framework for dansgaard-oeschger cycles. *Nature Reviews Earth & Environment*, 1(12), 677-693. doi:10.1038/s43017-020-00106-y
- Menviel, L., Timmermann, A., Friedrich, T., & England, M. H. (2014). Hindcasting the continuum of dansgaard-oeschger variability: Mechanisms, patterns and timing. *Climate of the Past*, 10(1), 63-77. doi:10.5194/cp-10-63-2014
- North Greenland Ice Core Project Members. (2004). High-resolution record of northern hemisphere climate extending into the last interglacial period. *Nature*, 431(7005), 147-151. doi:10.1038/nature02805
- Oeschger, H., Beer, J., Siegenthaler, U., Stauffer, B., Dansgaard, W., & Langway, C. (1984). Late glacial climate history from ice cores. *Climate Processes and Climate Sensitivity*, 299-306. doi:10.1029/gm029p0299
- Peltier, W. R., Argus, D. F., & Drummond, R. (2015). Space geodesy constrains ice age terminal deglaciation: The global ICE-6g_c (VM5a) model. *Journal of Geophysical Research: Solid Earth*, 120(1), 450-487. doi:10.1002/2014jb011176
- Peltier, W. R., Ma, Y., & Chandan, D. (2020). The KPP trigger of rapid AMOC intensification in the nonlinear Dansgaard-Oeschger relaxation oscillation. *Journal of Geophysical Research: Oceans*, 125(5). doi:10.1029/2019jc015557
- Peltier, W. R., & Sakai, K. (2001). Dansgaard-Oeschger oscillations: A hydrodynamic theory. *The Northern North Atlantic*, 423-439. doi:10.1007/978-3-642-56876-3_23

- Peltier, W. R., & Vettoretti, G. (2014). Dansgaard-Oeschger oscillations predicted in a comprehensive model of glacial climate: A “kicked” salt oscillator in the Atlantic. *Geophysical Research Letters*, 41(20), 7306-7313. doi:10.1002/2014gl061413
- Petoukhov, V., Ganopolski, A., Brovkin, V., Claussen, M., Eliseev, A., Kubatzki, C., & Rahmstorf, S. (2000). CLIMBER-2: A climate system model of intermediate complexity. Part I: model description and performance for present climate. *Climate Dynamics*, 16(1), 1-17. doi:10.1007/pl00007919
- Phillips, N. A. (1956). The general circulation of the atmosphere: A numerical experiment. *Quarterly Journal of the Royal Meteorological Society*, 82(354), 535-539. doi:10.1002/qj.49708235422
- Rahmstorf, S. (2002). Ocean circulation and climate during the past 120,000 years. *Nature*, 419(6903), 207-214. doi:10.1038/nature01090
- Rasmussen, T. L., & Thomsen, E. (2013). Pink marine sediments reveal rapid ice melt and Arctic meltwater discharge during Dansgaard–Oeschger warmings. *Nature Communications*, 4(1). doi:10.1038/ncomms3849
- Rasmussen, T. L., Thomsen, E., & Moros, M. (2016). North Atlantic warming during Dansgaard-Oeschger events synchronous with Antarctic warming and out-of-phase with Greenland climate. *Scientific Reports*, 6(1). doi:10.1038/srep20535
- Rooth, C. (1982). Hydrology and ocean circulation. *Progress in Oceanography*, 11(2), 131-149. doi:10.1016/0079-6611(82)90006-4
- Sadatzki, H., Dokken, T. M., Berben, S. M., Muschitiello, F., Stein, R., Fahl, K., ... Jansen, E. (2019). Sea ice variability in the southern Norwegian Sea during glacial dansgaard-oeschger climate cycles. *Science Advances*, 5(3), eaau6174. doi:10.1126/sciadv.aau6174
- Schneider, T., Bischoff, T., & Haug, G. H. (2014). Migrations and dynamics of the intertropical convergence zone. *Nature*, 513(7516), 45-53. doi:10.1038/nature13636
- Smagorinsky, J. (1958). On the numerical integration of the primitive equations of motion for baroclinic flow in a closed region. *Monthly Weather Review*, 86(12), 457-466. doi:10.1175/1520-0493(1958)086<0457:otniot>2.0.co;2
- Stocker, T. F., & Johnsen, S. J. (2003). A minimum thermodynamic model for the bipolar seesaw. *Paleoceanography*, 18(4), n/a-n/a. doi:10.1029/2003pa000920
- Timmermann, A., Gildor, H., Schulz, M., & Tziperman, E. (2003). Coherent resonant millennial-scale climate oscillations triggered by massive Meltwater pulses. *Journal of Climate*, 16(15), 2569-2585. doi:10.1175/1520-0442(2003)016<2569:crmcot>2.0.co;2

Tzedakis, P., Pälike, H., Roucoux, K., & De Abreu, L. (2009). Atmospheric methane, southern European vegetation and low-mid latitude links on orbital and millennial timescales. *Earth and Planetary Science Letters*, 277(3-4), 307-317. doi:10.1016/j.epsl.2008.10.027

Vettoretti, G., & Peltier, W. R. (2016). Thermohaline instability and the formation of glacial North Atlantic super polynyas at the onset of dansgaard-oeschger warming events. *Geophysical Research Letters*, 43(10), 5336-5344. doi:10.1002/2016gl068891

Vettoretti, G., & Peltier, W. R. (2018). Fast physics and slow physics in the nonlinear dansgaard-oeschger relaxation oscillation. *Journal of Climate*, 31(9), 3423-3449. doi:10.1175/jcli-d-17-0559.1

WAIS Divide Project Members. (2015). Precise interpolar phasing of abrupt climate change during the last ice age. *Nature*, 520(7549), 661-665. doi:10.1038/nature14401

Wolff, E., Chappellaz, J., Blunier, T., Rasmussen, S., & Svensson, A. (2010). Millennial-scale variability during the last glacial: The ice core record. *Quaternary Science Reviews*, 29(21-22), 2828-2838. doi:10.1016/j.quascirev.2009.10.013

Zhang, X., Lohmann, G., Knorr, G., & Xu, X. (2013). Different ocean states and transient characteristics in last glacial maximum simulations and implications for deglaciation. *Climate of the Past*, 9(5), 2319-2333. doi:10.5194/cp-9-2319-2013

Zhang, X., Lohmann, G., Knorr, G., & Purcell, C. (2014). Abrupt glacial climate shifts controlled by ice sheet changes. *Nature*, 512(7514), 290-294. doi:10.1038/nature13592

9. Appendices

Appendix A: Some technical information about SciNet

The following information comes from the official SciNet website, <https://www.scinethpc.ca/>.

SciNet is the supercomputing centre at the University of Toronto, and is funded by the Canada Foundation for Innovation, NSERC, the Government of Ontario, Fed Dev Ontario, and the University of Toronto. SciNet consists of various clusters, though this project only utilizes the main supercomputing cluster, the Niagara cluster. This cluster is made up of 2,016 nodes. Each node has 40 cores (either Intel Skylake cores at 2.4 GHz, or Cascadelake cores at 2.5 GHz), which results in a total core count of 80,640 cores for the entire cluster. Each node of Niagara has 202 GB of RAM, and the entire cluster has 6 PB of scratch and 3 PB of project space. On top of the Niagara cluster, SciNet also has a separate, tape-backed storage system that acts as a repository for archived data. This storage system is referred to as the High Performance Storage System (HPSS), and currently contains 9 PB of data. HPSS is used by this project to store archived data.

Some of these resources listed above were allocated for the project. For each 50-year run, the DO.noDD.fwf simulations were allocated 24 nodes with Skylake cores. With 40 cores per node, this totals to 960 cores. For each 50-year run, it took approximately 20 hours, meaning a total of 19,200 core-hours was taken per run. In terms of storage, each 50-year run produced 900 GB of data, which after compression into a netCDF format, shrinks to around ~325 GB of data.

Appendix B: Workflow for running simulations (Detailed Method)

Setting up simulation

First, a SciNet account was procured by registering with the Compute Canada Database (found here: <https://ccdb.computecanada.ca/security/login>) and requesting access to Niagara.

After the SciNet account was created, a copy of an existing model, the one used by Peltier et al. (2020), was made. This copying of the existing model and its relevant files was done for all three of the models used in this project.

After copying over the model, the environment configuration file (env_conf.xml) was modified. In the case of the project, the run types were hybrid, and started at year 2476. This is the point where it branches from the existing model that was copied over. The environmental configuration file is also where the length of each run was specified. Generally, each run was 50 years long, though at times when fine-tuning was needed (for example determining when to start adding freshwater forcing), this length was reduced to 25 years.

After that, many edits were made to the files in the build configuration directory to specify the details of the models. The technical details are below in Table B1.

Table B1: Specified build configuration parameters for project models

Filename	Parameter Name	Parameter Value	Reason for change
cam.buildnml.csh	ncdata	DO.1.noDD.2031.cam2.i.2476-01-01-00000.nc	Point to the location/name of the initial atmospheric conditions restart file.
cice.buildnml.csh	ice_in	DO.1.noDD.2031.cice.r.2476-01-01-00000.nc	Point to the existing restart file for simulated sea ice results.
pop2.buildnml.csh	ltidal_mixing	.false.	Turns off tidal mixing. This is a simplification as the tidal mixing regime is dependent on a modern bathymetry which doesn't align with LGM conditions (Peltier and Vettoretti, 2014).

	lbdl_diff	.false.	Turns off double diffusion mixing parameter (Peltier et al. 2020).
	bckgrnd_vdc1, bckgrnd_vdc2	0.524, 0.212	Sets a background vertical mixing that is a hyperbolic tangent in the vertical.
	lhoriz_varying_bckgrnd	.false.	Set it so that the horizontal background mixing does not vary.
	overflows_on, overflows_interactive	.false., .false.	Overflow parameters are to aid the flow of water, but are tied to present-day conditions, so turned off.
sfwf_formulation sfwf_data_type sfwf_data_inc sfwf_interp_freq sfwf_interp_type sfwf_interp_inc sfwf_restore_tau sfwf_filename sfwf_file_fmt sfwf_data_renorm(1) sfwf_weak_restore sfwf_strong_restore sfwf_strong_restore_ms	sfwf_formulation	'hosing'	Adds a specific amount of freshwater forcing defined by the sfwf_filename file and applies it at every ocean time step.
	sfwf_data_type	'monthly'	
	sfwf_data_inc	1.e20	
	sfwf_interp_freq	'every-timestep'	
	sfwf_interp_type	'linear'	
	sfwf_interp_inc	1.e20	
	sfwf_restore_tau	1.e20	
	sfwf_filename	'hosing_off.nc'	
	sfwf_file_fmt	'nc'	
	sfwf_data_renorm(1)	1.0	
	sfwf_weak_restore	0	
	sfwf_strong_restore	0	
	sfwf_strong_restore_ms	0	

This setup replicates the runs of Peltier et al. (2020), including the lack of freshwater forcing (note that the sfwf_filename in pop2.buildnml.csh refers to hosing_off.nc). When the simulation runs to a specific point in time where freshwater forcing should be introduced, this filename is changed to one with relevant forcing. The files used in this project were hosing_0.2sv.nc, hosing_0.1sv.nc, and hosing_0.01sv.nc for runs v1, v2, and v3, respectively. The area over which this forcing was introduced is shown in Figure 13, and the plot was generated using Panoply.

Processing Data

After runs start completing, postprocessing was done to make plots. For each batch of raw data, three programs were used to generate the data to be used in the plotted AMOC time series. First, the data was compressed using compress.sh. The compressed data was then converted to monthly data with the L2Series program. Afterwards, L3Series was run to convert the data to yearly averages. This creates the yearly netCDF files used in the data analysis.

These netCDF files are then copied over from SciNet so plotting of the data can be done. The main areas of interest from these data files are AMOC strength and temperatures in Greenland and Antarctica. The processing codes hosted on SciNet are all pre-existing scripts and were shared with this project by Dr. Deepak Chandan and can be provided upon request. The plotting scripts were adapted from code provided by Dr. Chandan or were specifically developed and examples are included in Appendix C.

Archiving Data

Once the data was processed, it was archived to HPSS. This was done by utilizing the ‘archive’ function from the cesmL1toHPSS.py script. This creates tar files for archiving that get stored on HPSS. Afterwards, utilizing the ‘clean’ function from the same script removes the original data and the tar files.

Appendix C: Code snippets for plotting

Importing packages/setting up environment:

```
%matplotlib inline
import matplotlib as mpl
from matplotlib import colors
from mpl_toolkits.basemap import Basemap
import matplotlib.pyplot as plt
import netCDF4 as nc
import numpy as np
```

Example code for plotting AMOC strength:

```
# Function to take decadal average of data (from Deepak)
def decadalavg(data):
    ret = []
    for i in range(len(data) // 10):
        avg = np.sum(data[i*10:(i+1)*10]) / 10
        ret.append(avg)
    return np.arange(len(ret)) * 10 + 5, np.array(ret)

# Load in file: example with v1
ncf = nc.Dataset("DO.noDD.fwf.v1.nc", "r")
fwfv1 = ncf["ocn/MOC_ATLN_max"][:]
ncf.close()

# Plotting AMOC series
plt.figure(figsize=(12,6))
ax = plt.gca()
x, avg = decadalavg(fwfv1)
ax.plot(x + 2475, avg, color="k", label="0.2 Sv FWF")

# Marking forcing period
plt.axvspan(2550, 2700, color="#E8E8E8")
plt.axvline(2550, linewidth=0.5, linestyle="--", color='k')
plt.axvline(2700, linewidth=0.5, linestyle="--", color='k')
plt.text((2550 + 2700) / 2, 15, "Forcing Period v1", color='k',
rotation=90)

# Labelling plot
ax.set_xlabel("Model years")
ax.set_ylabel('AMOC (Sv)')
ax.set_ylim([0, 50])
ax.legend(loc=9, ncol=5)
```

Example code for plotting NGRIP/EDML temperatures:

These plots follow the same logic as plotting the AMOC time series. They differ by loading in different variables from the netCDF files. To load in the temperature at the NGRIP and EDML ice core sites, we use:

```
ncf = nc.Dataset("DO.noDD.fwf.v1_temps.nc", "r")
fwfv1_ngrip = ncf["NGRIP/TREFHT"][:]
fwfv1_edml = ncf["EDML/TREFHT"][:]
ncf.close()
```

We also need to create a secondary y-axis to plot the AMOC strength along with the temperatures. This is done with:

```
ax2 = ax1.twinx()
```

Then the AMOC strength time series is plotted on ax2 rather than ax1.

Example code for plotting temperature anomaly map:

```
# Load in 2 periods to compare. Example uses the v3 stadial and
interstadial

#v3 interstadial
ncf = nc.Dataset("DO.noDD.fwf.v3.climatology.2700-2800.nc", "r")
atm = ncf.groups["atm"]
v3_is = atm.variables['TREFHT'][:]
ncf.close()

#v3 stadial
ncf = nc.Dataset("DO.noDD.fwf.v3.climatology.3350-3450.nc", "r")
atm = ncf.groups["atm"]
v3_s = atm.variables['TREFHT'][:]
ncf.close()

# Plotting
diff = v3_is-v3_s
m = Basemap(projection='cyl',llcrnrlat=-90,urcrnrlat=90, \
            llcrnrlon=0,urcrnrlon=360,resolution='c')
X,Y = np.meshgrid(lon,lat)
x,y = m(X,Y)
fig = plt.figure(figsize=(15,7))
m.drawcoastlines()
m.drawparallels(np.arange(-80.,81.,20.))
m.drawmeridians(np.arange(0.,360.,20.))
m.drawmapboundary(fill_color='white')
cs = m.contourf(x,y,diff,cmap='RdBu_r',vmin=-50, vmax=50)
# Adjust vmin/vmax based on what looks best
plt.title("Temperature anomaly between v3 interstadial and v3
stadial")
plt.colorbar(label='Temperature Anomaly (K)')
```

